minerals

MDPI

Article

Automated Gold Grain Counting. Part 2: What a Gold Grain Size and Shape Can Tell!

Réjean Girard *, Jonathan Tremblay, Alexandre Néron, Hugues Longuépée and Sheida Makvandi

IOS Services Géoscientifiques Inc., Chicoutimi, QC G7J 3Y2, Canada; jtremblay@iosgeo.com (J.T.); neron.alex@iosgeo.com (A.N.); hlonguepee@iosgeo.com (H.L.); sh.makvandi@gmail.com (S.M.)
* Correspondence: rejeang@iosgeo.com

Abstract: Glacial drift exploration methods are well established and widely used by mineral industry exploring for blind deposit in northern territories, and rely on the dispersion of mineral or chemical signal in sediments derived from an eroded mineralized source. Gold grains themselves are the prime indicator minerals to be used for the detection of blind gold deposits. Surprisingly, very little attention has been dedicated to the information that size and shape of gold grain can provide, other than a simple shape classification based on modification affecting the grains that are induced in the course of sediment transport. With the advent of automated scanning electron microscope (SEM)-based gold grain detection, high magnification backscattered electron images of each grain are routinely acquired, which can be used for accurate size measurement and shape analysis. A library with 88,613 gold grain images has been accumulated from various glacial sediment surveys on the Canadian Shield and used to detect trends in grains size and shape. A series of conclusions are drawn: (1) grain size distribution is consistent among various surveys and areas, (2) there is no measurable fine-grained gold loss due to natural elutriation in ablation or reworked till, or during the course of reverse circulation drilling, (3) there is no grain size sorting during glacial transport, severing small grains from large ones, (4) shape modification induced by transport is highly dependent on grain size and original shapes, and (5) the use of grain shape inherited from neighboring minerals in the source rocks is a useful feature when assessing deposit types and developing exploration strategies.

Keywords: gold; till; glacial sediments; gold grain morphology; gold grain size; automated SEM; gold exploration; drift prospecting

Citation: Girard, R.; Tremblay, J.; Néron, A.; Longuépée, H.; Makvandi, S. Automated Gold Grain Counting. Part 2: What a Gold Grain Size and Shape Can Tell!. *Minerals* **2021**, *11*, 379. https://doi.org/10.3390/min11040379

Academic Editors: Derek H. C. Wilton and Gary Thompson

Received: 19 February 2021
Accepted: 30 March 2021
Published: 2 April 2021

1. Introduction

Gold grain dispersion in secondary environment is an extensively used exploration method for tracing blind gold deposit, especially in glaciated terrain [1–5]. The concept is that gold almost exclusively occurs as native metal in rocks, and that these metal particles are malleable but nearly unbreakable and staggeringly resistant to alteration and weathering. Therefore, they survive erosion and transport, and are preserved in the resulting sediments [3–5]. Gold being malleable, it has long been recognized that grains freed in the secondary environment undergo modification of shape through transport, which led the industry to estimate these attrition feature to evaluate distances to the source [6]. There is also a strongly rooted belief that small gold grains are severed from large ones in the course of transport, and should be interpreted differently [7]. However, the validity of these hypotheses has never been rigorously tested due to the lack of dependable data, and despite the extensive use of gold dispersion in sediments by explorationists [3], very little attention has ever been dedicated to the accurate characterization of the gold grains.

Historically, gold grains size was estimated by mineralogists under an optical microscope [8], and shape was characterized as "pristine," "modified" or "reshaped" [6]. The shape classification was initially developed from high resolution back-scattered electron (BSE) images and is based on vague criterions, the use of which relies upon mineralogist

interpretation. However, during routine sample processing [4], this interpretation is made while the grains are being sorted under low magnification optical stereomicroscope. It is, therefore, subjected to the mineralogist's own perception based on low resolution images. Furthermore, accurate relation to transport distances or processes and its variability has never been documented. This information, usually released only as grain counts by the laboratory [4], without providing images, can hardly be verified by the user, who will use it for decisions regarding costly exploration programs. Although plenty of case studies where the method has been efficient at pointing to mineral deposits have been published [9–12], there is an abundant number of surveys that did not work and, consequently, were not publicized. As described in a companion paper [13], evaluating the size and shape of grain with an optical microscope is plagued with difficulties, so the results can be biased and inconsistent, if not blatantly wrong, and thus, misleading if used for exploration. This lack of robust studies led the industry to use "rules of thumbs," many of which are poorly supported and will be dismissed in following pages. For example, many explorationists consider that minute gold grains are more dispersed in the secondary environment than large ones, and should be disregarded; a belief that typically leads to poor exploration decision.

Gold grains are surprisingly abundant in glacial sediments, with an overall background of 5–10 grains per samples [10,14,15]. However, the apparent lack of characteristics (size, shape, chemical composition, trace element contents, colors, attachments etc.), gives the impression that these can only be used as an intensity marker, not as a metallotecte fingerprints. To circumvent the apparent incapacity to characterize the source of gold grains, a panoply of associated indicator minerals, considered as fingerprint of various gold deposit type, were tentatively developed [16–20]. For example, scheelite is common in orogenic gold deposit [16], tourmaline is suggestive of intrusion-related deposit [17], grossular or andradite are associated with porphyries [21], etc. These approaches are typically limited by the cost of conducting elaborate indicator mineral studies (2–3 × the cost of extracting gold grains), which need to be conducted on a larger (250–1000 µm) size fraction of the sample. Additionally, the use of associated indicator minerals is hindered by several issues; first, most indicator minerals are naturally scarce, causing representativeness issues (e.g., dumortierite in orogenic gold deposits). Second, some minerals are difficult to differentiate during visual sorting (e.g., tourmaline versus hornblende). Third, the impossibility to efficiently discriminate grains with meaningful chemistry from usual grain of the same species (e.g., rutile [22] or magnetite [23–27]) by visual sorting is an issue that requires a massive number of grains to be analyzed with an electron microprobe (EMP) or by laser ablation coupled to a plasma mass spectrometer (LA-ICP-MS). Fourth, the so-called distinctive chemistry was typically characterized from mineralized occurrence only, and therefore, the background signature is poorly documented (e.g., magnetite [23,24,28]). Fifth, many of these minerals are not resistant in the secondary environment (e.g., sulfosalt, arsenopyrite [29]) or cannot be efficiently concentrated (e.g., ankerite, albite, tourmaline). Finally, the presence of some minerals can be more easily detected by a simple chemical analysis. For example, arsenopyrite or chalcopyrite are commonly associated with gold mineralization, but since arsenic or copper are not partitioned into common mineral, but almost exclusively in sulfides or sulfosalts, their abundance can more easily be detected by simple aqua-regia induced plasma (ICP) spectrometry [15,29]). Studying these indicator minerals is of obvious interest with regards to characterizing the signature of a deposit but of limited applicability in exploration. Gold remains the best indicator mineral to be used for the detection of gold deposit, on the simple basis of its contrasting signal to background abundance and ease to extract and count [13]. Carlin type might be the exception, where most gold grains are reported too small to be recovered by the current method.

With the advent of SEM-based automated gold grain identification procedures, high magnification BSE images are acquired for each grain and from which accurate size morphology measurement can be made. A semi-quantitative chemical analysis is computed from an EDS spectrum, the use of which is described in a companion paper [13]. As a

result, images and the analysis of more than 100,000 gold grains, accumulated from dozens of private glacial sediments surveys across the Canadian Shield (Figure 1), can be used to tests the aforementioned hypotheses. More than half of these surveys were conducted by the same group of trained quaternary geologist, and includes a systematic and detailed description of samples and landscape. The database contains a wealth of information that can be used to understand the grain dispersion process and provides clues regarding the source rocks. Such database has never been accumulated before, and therefore, no comparative studies are available. Characterization of the geological environment, metallogenic significance, and information pertaining to erosion and transports processes are still embryonic, but an exploratory data analysis of the database is conducted in order to outline relations between grains, sedimentary process and source rocks. However, sensitive information relevant to mineral exploration from the various surveys cannot be disclosed, being of private nature.

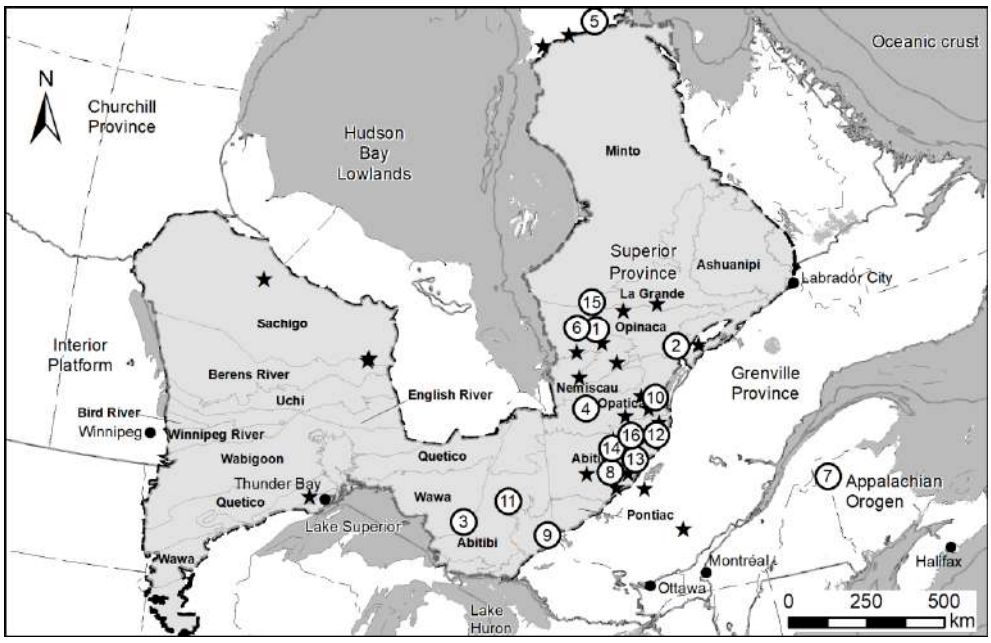

Figure 1. Location of the various till sampling survey used in the current study. Numbered projects refer to surveys listed in Table 1, in the order they are listed.

Table 1. Statistics on the measured long axis of gold grains from lodgment tills of 16 recent sampling programs. Grain size distribution is assumed as log-normal; the log-mean, log-standard deviation, asymmetry coefficient (skewness) and kurtosis were calculated on the logarithm (Log_{10}) of grain size. The constancy of the distribution among projects is discussed in the main text. Still, due to the large number of grains involved, the difference between the means is still statistically significant according to a Student's t-test, and cannot be caused by the variance of each population.

Survey	Count	Mean	Std-Dev	Median	1st Centile	99th Centile	Log-Mean	Log-Std-Dev	Asymetry	Kurtosis
Opinaca #1, QC	243	35.0	36.7	28.3	9.6	172	1.45	0.244	1.11	3.06
Eastmain, QC	3156	37.5	22.6	32.3	11.0	125	1.52	0.216	0.32	0.48
Wawa, ON	6501	36.1	32.3	28.5	8.9	183	1.47	0.249	0.71	1.71
Nottaway, QC	737	42.8	25.3	36.5	11.8	141	1.57	0.229	0.17	0.19
Cape Smith, QC	11,937	31.9	23.1	26.5	9.6	115	1.44	0.224	0.53	1.08
Opinaca #2, QC	782	38.6	27.2	30.8	10.9	155	1.51	0.241	0.57	0.41
Appalachian, NB	137	38.8	23.2	33.5	13.1	133	1.53	0.217	0.36	0.34
Abitibi #1, QC	343	38.6	23.6	32.8	11.9	141	1.53	0.219	0.34	0.56
Temiskaming. ON	355	43.9	27.0	37.4	12.5	146	1.58	0.234	0.16	0.46

Table 1. *Cont.*

Survey	Count	Mean	Std-Dev	Median	1st Centile	99th Centile	Log-Mean	Log-Std-Dev	Asymetry	Kurtosis
Frotet, QC	608	41.3	25.2	35.0	13.0	138	1.55	0.223	0.42	0.14
Abitibi, ON	4025	39.3	44.2	29.6	9.5	189	1.50	0.263	0.79	1.70
Chibougamau, QC	4742	42.2	37.3	34.7	12.6	160	1.56	0.225	0.65	1.47
Urban-Barry, QC	809	34.6	22.3	28.9	9.6	130	1.48	0.227	0.35	0.51
Abitibi #2, QC	504	36.4	22.5	30.6	11.2	111	1.50	0.218	0.53	0.46
LaGrande, QC	253	33.2	24.0	28.2	8.9	119	1.45	0.233	0.29	1.11
Northern Abitibi, QC	225	35.2	30.2	27.9	9.9	197	1.46	0.247	0.82	1.84
Total	35,357									
Average		37.8	27.9	31.3	10.9	147.2	1.5	0.2	0.5	1.0
Std-dev		3.51	6.53	3.34	1.49	26.71	0.04	0.01	0.26	0.80
Coef.Variation		9.3%	23.4%	10.7%	13.7%	18.1%	2.9%	5.9%	50.9%	82.6%

The chemistry and texture of indicator minerals are routinely used to characterize their source rock and to draw conclusion about the metallogenic environment they originate from [20,25–27,30–36]; gold grain characteristics (e.g., shape and chemical signature) are indicative of their source [3,6,37–42]. It is assumed that gold grains have distinctive characteristics related to the mineralizing environment [43–53]. The presence or abundance of such characteristics [47,48] enables source discrimination and indicates if the grains contained in a specific, anomalously rich sample are part of the regional signal or have a signature suggestive of a distinct local source [3]. These signatures are useful to discriminate the footprint of various sources among a regional survey [10]. However, such research remains hampered by the lack of systematic information on gold grain characteristics and the variability among types of deposit.

2. Database and Acquisition Procedures

The database (Table S1, Supplementary Materials) used for the current study is a private set of data acquired by the authors since the inception of the SEM-based automated gold grain procedure in 2015. Data are the property of numerous clients, and although most of it is available in public reports (assessments or governmental reports), the origin of samples, their location and meaning in regard to local exploration remains sensitive and shall not be disclosed.

The database, as of 11 January 2021, included 88,613 grains that were extracted from 8107 samples of glacial or periglacial sediments from 47 different surveys across the Canadian Shield (Figure 1). Also available are 9970 grains that were recovered from 30 metallurgical tests, which provide some information about characteristics of grains in their respective host deposits. Most of the surveys are located in the Abitibi and James Bay area of the Superior Craton, although some are from Archean terrain of Manitoba, lower Proterozoic Cape Smith belt in Northern Québec as well as late Paleozoic Appalachian areas from New-Brunswick. About 61% of the samples were collected by the IOS crew of trained quaternary geologists and were described in details, according to a uniform protocol. The remaining 39% of samples were collected and submitted by third parties according to industry standard protocol, but typically lacking detailed description. The majority of samples (95%) were collected from the surface with a hand shovel or small hydraulic excavator at a typical depth of 1–2 m, below the ferruginous B pedologic horizon. About 5% of the samples were collected at greater depth, either with the use of large hydraulic excavator, reverse circulation drilling or Sonic overburden drilling. Number of samples and gold grains available in the database are provided by sediment types in Table 2. Descriptions of samples submitted by third parties were validated by technicians in the laboratory and through the grain size distribution measurements (Figure 2).

Table 2. Statistics on samples and gold grains available in the database, according to sediment types. Number of metallurgical tests and gold grains recover from these are provided for comparison.

Sediment Type	Samples		Gold Grains		Grains/Samples
	Number	%	Number	%	
Total	8107	100%	89,613	100%	11.1 gg/s
Undiscriminated tills	3568	44%	27,634	28%	8.0 gg/s
Lodgment tills	2151	26.5%	35,086	35%	16.3 gg/s
Hybrid tills	841	10%	11,967	12%	14.2 gg/s
Ablation tills	1059	13%	13,275	13%	12.5 gg/s
Reworked tills	79	1%	920	1%	11.6 gg/s
Diamictons	28	0.5%	291	0.3%	10.4 gg/s
Fluvioglacial	364	4.5%	435	0.4%	1.2 gg/s
Alluvium and beach sand	17	0.2%	5	0.0%	0.3 gg/s
Metallurgical tests (Rocks)	30		9970		

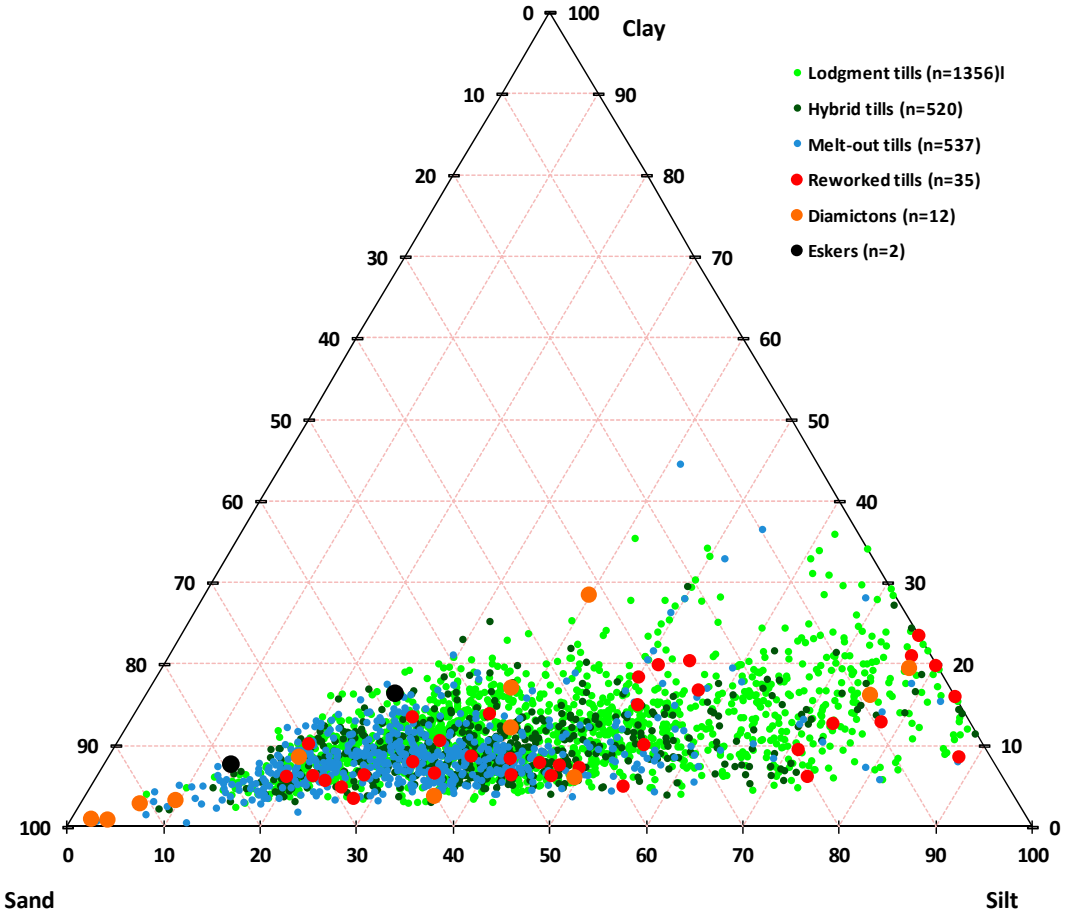

Figure 2. Sand, silt and clay proportions in 2462 till samples from northwestern Québec and northeastern Ontario. Particles larger than 1 mm were excluded, their proportion being too erratic. Grain size distribution is obtained from a laser dispersion grain sizer (Fritsch Analysette 22, using the Fraunhofer equations. While the clay (−4 µm) to silt (4–63 µm) ratio is quite constant, the sand (63–1000 µm) abundance increases from lodgment till, to hybrid till to fusion (melt-out) till. Reworked material, diamicton and fluvioglacial show large scattering.

All samples were processed with a proprietary procedure that includes wet sieving at 1 mm, gold grain concentration with a fluidized bed, dry sieving at 50 µm with a woven mesh, conventional sorting of the +50 µm size fraction for gold grains and automated detection and analysis of the −50 µm grains [13]. Automated sorting was either conducted with the use of ARTGold™ SEM-based scanning routine implemented on a 2013 Zeiss EVO-MA-15-HD-LaB_6 (Carl Zeiss AG., Cambridge, UK) equipped with an Oxford Instrument X-Max-150 energu dispersive detector (EDS) (Oxford Instrument, plc, Abingdon, UK) and a 2018 Zeiss Sigma 300-VP-FEG equipped with an Oxford Instrument Ultim-Max 170 EDS detector, or optical ARTPhot scanning routine implemented on a motorized Zeiss Axiozoom V16 microscope (Carl Zeiss AG., Oberkochem, Germay) plus SEM validation [54,55]. Both optical and SEM methods yield very similar results, except for grains smaller than 10 µm. Scanning is performed on material that is dusted on the sample holder, and not cast in polished epoxy. Dusting material as a monolayer on the sample holder is preferred to embedding it in epoxy and polishing since the purpose of the method is to count all grains initially present in the sample, and the embedding–polishing process inexorably expose only a limited portion of the concentrate [13,56].

SEM scanning is based on back-scattered electron image analysis, where particles with a minimal brightness and contrast corresponding to an approximate density of 5 g/cm^3 are detected. The threshold is set to avoid detecting monazite, which is ubiquitous by the thousands in the heavy mineral concentrate (HMC) and hinders the duration of the data acquisition. A routine built on the Feature module of Aztec 4.2 software (Oxford Instruments, Abingdon, UK) acquires the coordinates of the grains on the sample holder, and triggers the acquisition of a swift EDS spectrum of 300,000 effective counts that is deconvoluted into a semi-quantitative chemical analysis. Issues cause by acquiring the EDS spectrum on non-polished surface is discussed in a companion article [56]. The mineral species is classified based on its chemical composition with a cladogram that tags the particles into gold, platinum group minerals or various other heavy minerals (scheelite, wolframite, galena, bismuthides and tellurides, columbotantalite, U-Th minerals etc.). Once all programmed surfaces are scanned, a second semi-automated routine is run, which acquires a high magnification BSE image (image dimensions of 144 µm × 108 µm, 0.14 µm/pixel) of each particle tagged as gold or PGM grains and prompts the operator to confirm location of a spot EDS analysis based on 500,000 effective counts [56]. The tagged high-resolution image, EDS spectra and analyses are stored in a database.

2.1. Grain Size Measurement

Following high-resolution BSE image acquisition, each gold grain is segmented from image background and size is measured based on a pixel resolution of 0.14 µm. Size is expressed as the maximum length (length of the enclosing rectangle, not as the horizontal width or the longest ferret), width (width of the enclosing rectangle measured orthogonal to the maximum length), area (representing the number of included pixels and converted into $µm^2$) and equivalent circle diameter (calculated from the area). The limits of the grains are set at the maximum gradient closest to background brilliance. Pixels encompassing more than one mineral phase, typically at the edge or within the particle, are included and no grain boundary attrition or expansion is made. Size measurements, thus, have a precision in the order of 0.2 µm, assuming the grain is entirely exposed. No stereological correction is needed since the grains are totally visible and not embedded in epoxy to be partly exposed by polishing. Dusted material is preferred to epoxy cast and polishing since it exposes the entire outline of the grain, compared to a section only for cut and polished grains. The only limitation on size measurement with dusted material is if the grain is hidden underneath another or if there is a coating attached to the grain. Since the detector diode is located on the nose of the hyperconical lens, no shadowing issue is present.

Gold grain size distribution is bounded by two instrumental limitations. Grains larger than 1 mm, although expected to be very rare, are removed in the course of initial sample sieving. Inversely, grains smaller than 20 µm experience a recovery collapse during

gravimetric concentration [13], so their abundance in the concentrate is not representative of their abundance in the source material. The grain size distribution is then controlled by the lognormal grain size distribution in the source rocks, factored by the recovery function of the process. Measurement of the size is not instrumentally limited, since the image resolution of 0.14 µm is approximately 100 time smaller than the smallest grain expected to be recovered.

Tests were conducted to measure grain abundance and size with X-ray tomography [14]. Despites some advantages, practical application of the technique is limited due to the required acquisition and computing time if a sub-micrometer resolution is needed.

Gold grains' size was also extracted and measured for material from mineralized rocks in the course of various metallurgical tests. The material was milled sufficiently to liberate the gold, either in laboratory or in a mine concentrator. The material was the feed (unprocessed milled rock), the concentrates or the tails of the tests. Consequently, biases were induced by metallurgical testing, causing discrepancies towards very small or large grain abundances that more or less compensate each other if mixed into a single grain population. These grain size distribution curves differ from those measured from petrographic studies [13] involving only liberated grains and being affected by the instrumental recovery factor, and thus, depleted in the −20 µm range. The original morphologies of gold grains were partly preserved despite the aggressive milling process, which tends to round and "reshape" grains such as those that underwent long transport in sediments [57–64]. This set of reference gold grain is biased and imperfect, but shows size distributions that are similar to what is measured in glacial sediments.

Measurements on grains from a variety of till surveys (Figure 3) conducted in rigorously similar conditions indicate that grain size distribution is surprisingly constant, regardless of the survey location, regional geology or expected deposit types. Statistics on grains from lodgment tills of 16 different surveys (Figure 1), for which sampling and processing protocols were tightly monitored, indicate a coefficient of variation on the average or median grain size that is lesser than 10% (Table 1). The grain size distribution is assumed to be log-normal [65,66]; the statistics of the logarithm of the size were computed and indicate the various populations as being even more similar, with the variation coefficient on the log-average being less than 3%. Skewness (2nd moment) and Kurtosis (4th moment), or tailness, suggest that large grains are proportionally over-represented, as expected considering the recovery failure of small grains. This indicates that grain size distribution is not discriminating with regard to source material or deposits, to a certain extent.

Gold being malleable, grains cannot be fragmented, and their volume is expected to remain rather constant through the milling and liberation process. Thus, grain size distribution in naturally milled material, such as lodgment till, is expected to represent the one in source rocks [3,6,47,61], except for large platy or elongated grains that are likely to be rounded through transport, thus slightly reducing their apparent size. These distributions are effectively consistent with the one obtained from milled mineralized rocks (Figure 4), with a nearly identical average (reduced centered 90%), standard deviation and median.

Grain size distribution can be modified through natural elutriation along the various processes affecting the sediments once the source rock is eroded [3,64–67]. Although minimal in lodgment till, this elutriation is expected in sediments that have been in contact with running water, or more rarely wind. If a material has been elutriated of its fine fraction, fine gold grains are expected to wash away as well. Any contact of the rock flour from the lodgment till with meltwater is then expected to induce elutriation of fine gold, and the grain size distribution to be skewed toward larger particles. Fusion (melt-out or ablation) tills, which typically lay on top of the lodgment tills, originate from material from the lodgment till that was incorporated in the ice, and are deposited during ice melting [68]. Fusion tills are, thus, dominantly sandy, partly cleaned of their clay and silt content (Figure 2). Similarly, till material that has been in contact with post-glacial lacustrine, marine or alluvial environments was put in contact with water, and is

susceptible to be sorted. Fine gold particles are then expected to wash away, leaving a coarser size distribution.

Size distributions were calculated for gold grains recovered from various types of sediments, regardless of the surveys they originate from (Figure 4). Gold in basal till has a median size of 28 µm, while those from fusion till, hybrid tills (mixture of lodgment and fusion tills) or tills that were reworked by contact with water all show a median of 32 µm. The differences between the various types of glacial sediments, within the range of the current recoveries, are dim and of similar magnitude as what would be noted between projects for the same type of sediments. This suggests that only grains smaller than what can efficiently be recovered was efficiently elutriated. The differences in gold grain counts and size distribution between lodgment and other tills were not pronounced, and both can be considered as a single population in assessing a survey. Still, care must be taken since the dispersion distance can be different between both types of sediments, with lodgment tills assumed to be more proximal than fusion tills. In contrast, grain size distribution in sediment that underwent contact with energetic environment, such as eskers, fluvioglacial materials, alluviums or beaches, have a drastically coarser size distribution (Figure 4). Glaciomarine or glaciolacustrine sediments deposited in calm environment inversely contain only the smaller grains, unlikely to be counted due to instrumental recovery limitations.

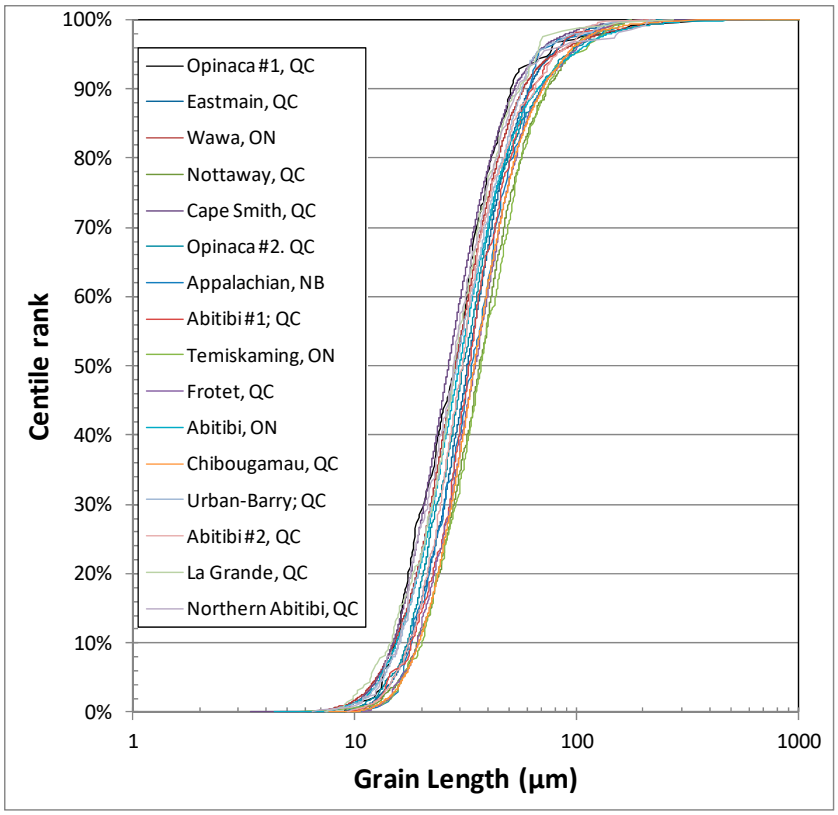

Figure 3. Gold grain size cumulative distribution plot for 16 recent sampling programs (Figure 1) where samples were collected with hand shovel by the same crews. Only genuine lodgment tills were included to ensure homogeneity. The surveys are dominantly located within the Superior Archean craton, testing for orogenic gold deposit in northwestern Québec and northeastern Ontario. One survey (Cape Smith) is located in the early Proterozoic mobile belt, while another (Appalachian) is located in Paleozoic terrain. All curves are very similar, parallels, with less than 10% variation of their mean, or 3% of the mean of the logarithm of the grain sizes. This is suggestive that gold grain size distribution is not significantly influenced by their source or metallogenic context. Severe divergence of such curves would be indicative of laboratory recovery issue or sorting in the sediments.

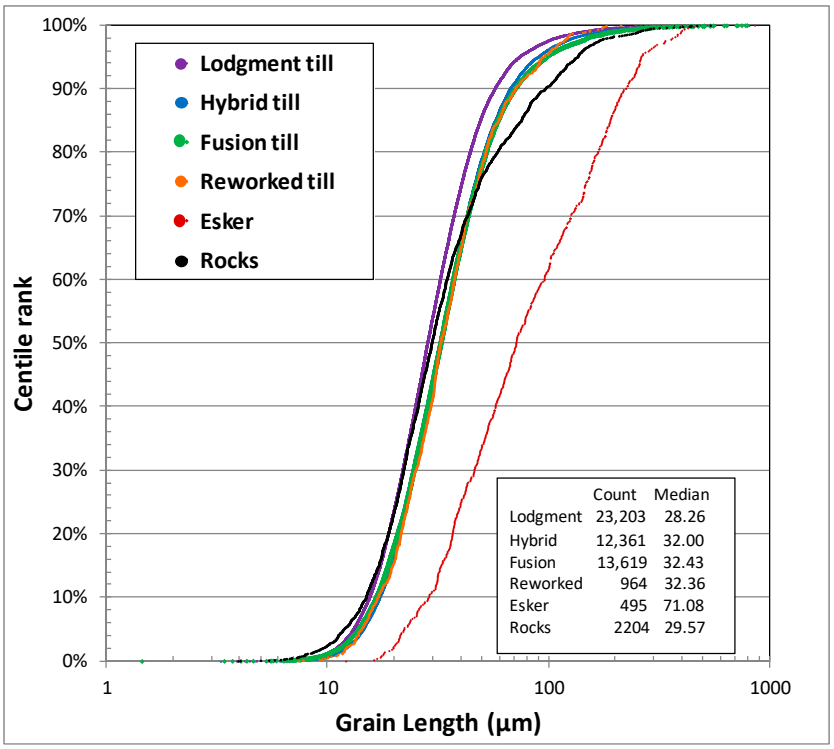

Figure 4. Gold grain size cumulative distribution plots according to sediments types. All samples were collected with a hand shovel by the same crew and sediment type is considered as properly classified. It can be noted that gold grains from lodgment tills are slightly finer than other types of sediment. Other glacial sediments that underwent contact with melt water, such as hybrid, fusion and reworked tills, are slightly coarser than those from lodgment tills, suggesting limited elutriation of the finest particles. Inversely, grains recovered from eskers or fluvioglacial sediments are distinctively coarser, suggestive of severe elutriation of fine grains. The black curve is for grains recovered from mineralized rocks though various metallurgical tests. Minute grains as well as grains larger than 40 µm are overrepresented compared to till, likely due to bias induced by the tests. However, the median grain size in rock remains similar to the one in the lodgment till.

Similarly, elutriation of minute gold grain is expected if sampling is conducted in water medium, such as reverse circulation (RC) drilling. Still, the grain size distribution of grain recovered from RC drilling does not shown bias when compared to samples recovered by Sonic drilling (a drilling method enabling the recovery of unperturbed unconsolidated sediments) or by hand shovel near the surface (Figure 5).

Since small grains are not significantly elutriated from the various types of sediments, it is expected that their displacement would be cohesive with the rest of the sample material. If they behave cohesively with the rest of the sample, they have a similar transport distance than their larger counterparts, as long as they are not affected by energetic alluvial processes. Consequently, samples that represent material from a distant regional source are expected to preserve their gold grain size distribution compared to proximal samples taken directly down-ice from a source.

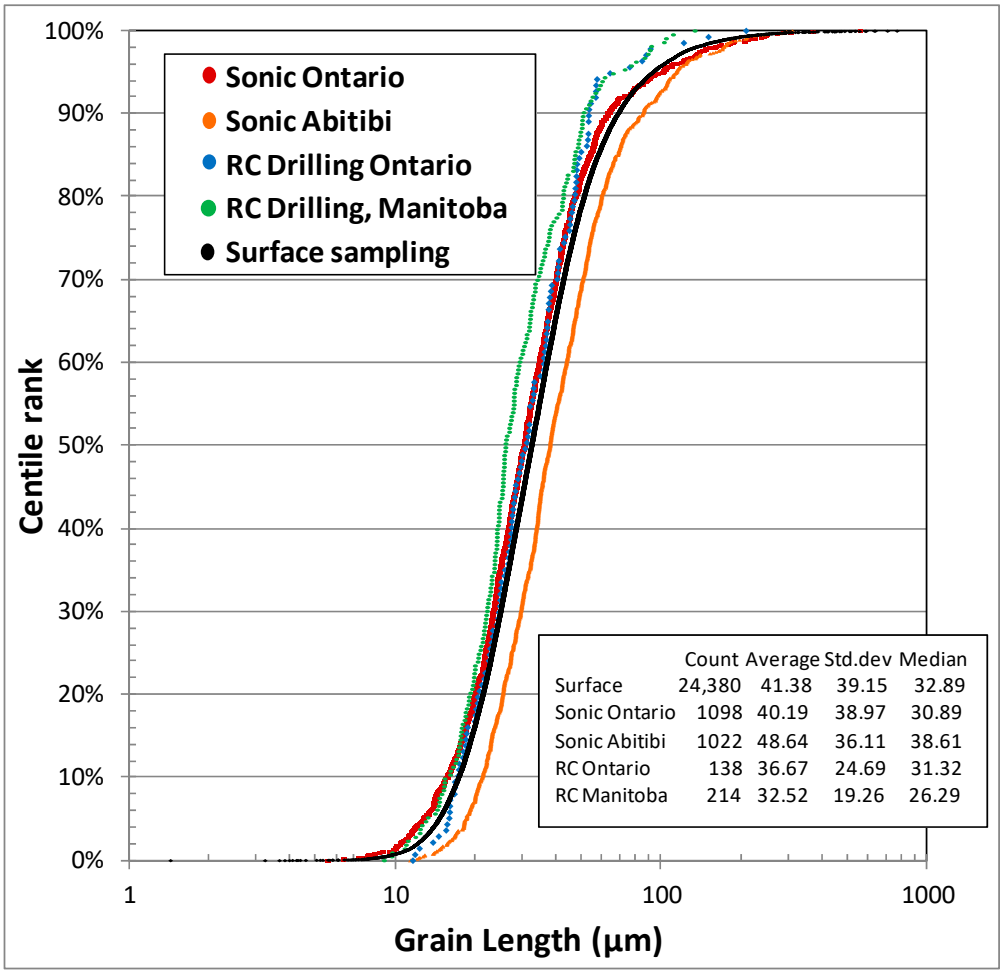

Figure 5. Gold grain size cumulative distribution plots according to sampling procedures. No significant difference is noted between samples collected from surface with a hand shovel, unperturbed core samples collected by Sonic drilling, and slurry generated by reverse circulation (RC) drillings. Material collected from RC drilling, although affected by severe mud elutriation, do not experience significant small gold grain losses at the scale of what can be recovered by the fluidized bed.

2.2. Shape Analysis

The interpretation of the gold grain shape is considered by many in the exploration industry as essential information to be collected, as it is widely used for transport distance assessments [6,42]. Shape classification used by the industry follows the initial scheme introduced by DiLabio [6] and perpetuated by commercial laboratories [4]. The grains are classified into (1) "pristine or intact" grains that retained their initial morphology as they were in the source rocks. These grains are typically characterized by smooth surface, complex shapes and sharp edges; (2) "modified" grains show evidences of attrition induced by transport during which they interacted with other particles or evidence of silver dissolution. They are characterized by less complex shapes, blunted edges and frosty surface; (3) "reshaped" grains typically lost all evidences of their original shapes, and are typically rounded with a pitted surface.

Although initially documented from high-resolution SEM images, routine shape interpretation is usually conducted with the help of optical stereomicroscope under limited magnification (16× to 40×) [13]. The three categories are not neatly limited and form a continuum of textures and shapes. A grain with an imperfectly developed texture can easily be classified as one or another shape (Figure 6), despite mineralogist training and even with the use of high-resolution BSE images. Consequently, the accuracy of this information is limited by both the image quality and the mineralogist's bias. Although

large grains are expected to be properly classified, small grains are difficult to assess and the misclassification rate is likely high. The magnitude of these biases has apparently never been assessed and is not available to data end-user. Still, this information, or the ratio of "pristine" to "modified" grains, is routinely used for exploration decision making.

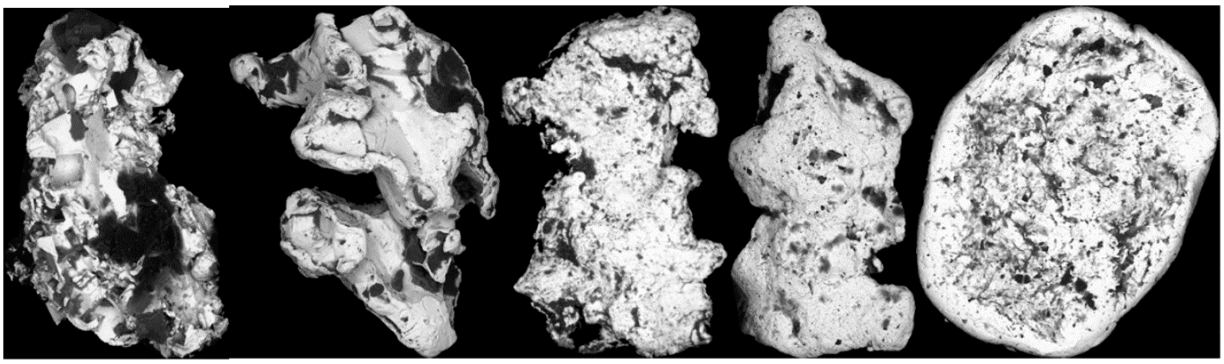

Figure 6. Examples of gold grain showing the continuum of shapes between "pristine (intergranular)" (**left**), "modified" (**center**) and "reshaped" (**right**). The grains in between can be classified as either neighboring class by different mineralogists, leading to discrepancies in the class counts. All grains are approximately 200 μm in length.

Since the inception of the automated SEM-based routine, high-resolution BSE images (500× to 2000×) are acquired and used for shape interpretation. Image acquired on dusted grains is preferred to those from polished surfaces, since it provide insights on the topography and texture at the surface of the grain. Third dimension reconstructions of the grains were tested using X-ray tomography, stereoscopic SEM images and Z-axis stacking with a motorized optical microscope [69], but are too time consuming to be deployed for routine surveys.

Up until 2017, morphofacies were interpreted from the BSE image by a trained geologist, and counter-verified by a second geologist, image per image. Since typical sediment samples contain tens of grains, and surveys may count them by the thousands, classifying each of the grain is a tedious task, prone to inconsistencies.

In 2018, a deep deconvoluting neuron-network image classification routine, based on Google's Inception V4, was developed for the classification of grains into morphofacies (ARTMorph routine) [70]. Mosaics of grains are assembled per morphofacies (Figure 7) and results are validated by a geologist, after which they are added to the database. The system has initially been trained on the image of grains unequivocally classified by geologists, and is regularly retrained to improve its performance. The misclassification rate of the routine is estimated at approximately 10%, better and more consistent than what most geologists can achieve [71].

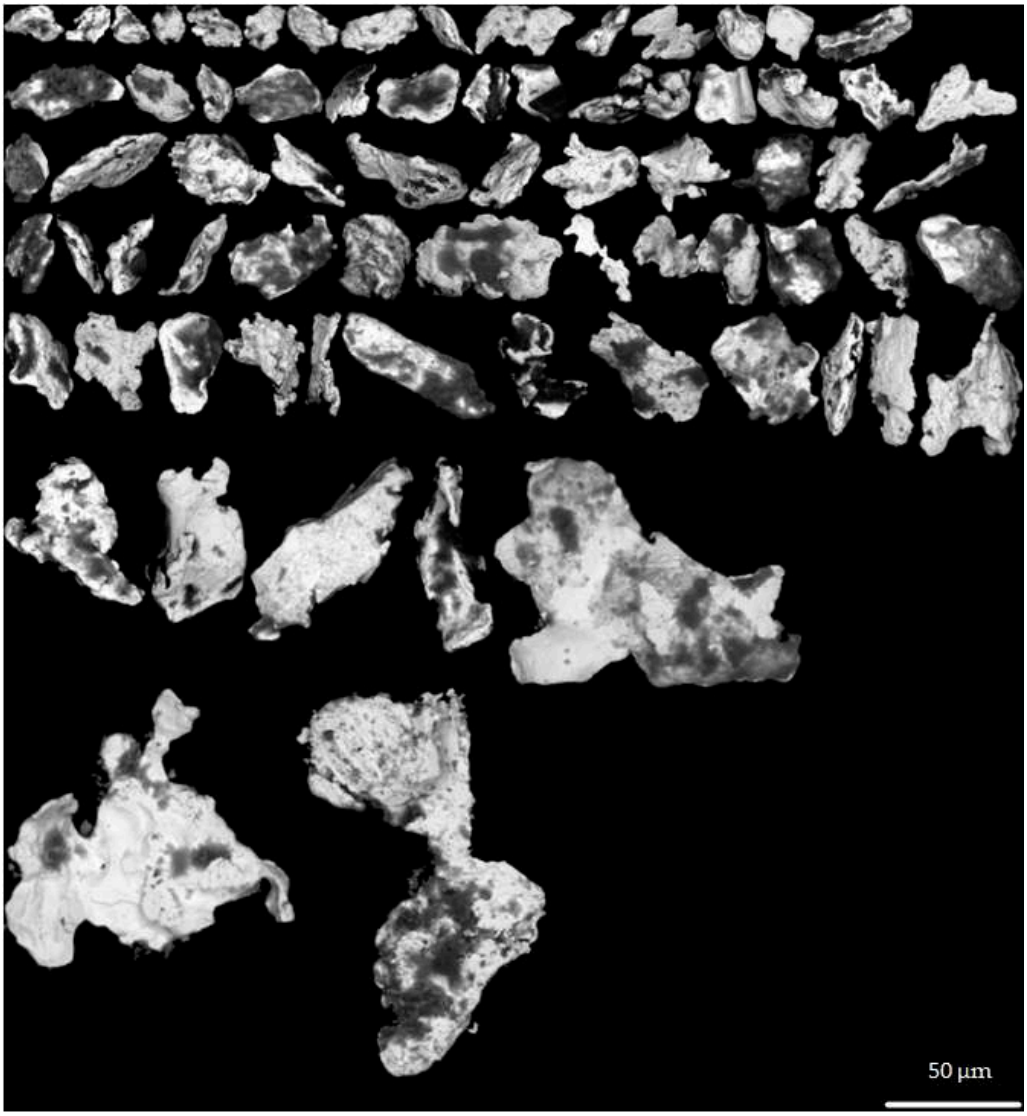

Figure 7. Example of a mosaic of "remobilized" grains generated automatically from a small glacial sediment survey from northern Abitibi, Québec. The shape classification has been performed with a CNN routine (ARTMorph).

More elaborate shape classification schemes were introduced in literature [39,72–74]. Most of these are purely descriptive (e.g., cornflakes, spherules, etc.), and were not adopted by the industry. Early in the development of the automated procedure, the authors noted that some shapes were recurrent among the "pristine" grains, shapes that were preserved as palimpsest in "modified" or even "reshaped" grains. A classification scheme has been elaborated for such "pristine" grains based on the relation between the grains and their neighboring minerals in the host rock. Four categories were introduced:

A: "Crystalline" grains (Figures 8A and 9) are those for which the shape is dictated by the cubic crystalline structure of the mineral. These can be nice cubes, tetrahedrons, dodecahedrons or complex crystals that can be stubby or highly elongated, twinned or forming complex dendrites. In most instances, only part of the grain developed such crystalline facets. To develop such crystalline habits, the grain must have grown without hindrance, either in voids or more commonly in contact with minerals that grew simultaneously, but with a lesser crystalline strength, such as in quartz or carbonate veins.

B: "Mutual" grains (Figures 8C and 9) are the inverse of the crystalline, in the sense that they grew alongside minerals with which they developed mutual relationship. This requires that the gold and its host grew coevally with similar crystalline strength. These

are typically small, simple in shape, bulbous and rounded, lacking sharp edges. They are interpreted as former gold droplets in sulfides.

C: "Intergranular" grains (Figures 8B and 9) are typically large and complex in shape, but lacking crystalline facets. Their shape is dictated by neighboring minerals, and large grains are then molding or infilling the joints between these. The shapes can be complex, with appendices, flaps and bulbs, and display curved smooth surfaces and sharp edges. Small intergranular grains form a continuum of shape with crystalline or mutual grains. They are interpreted to have grown dominantly between silicate grains, and are dominantly found in polymineralic silicate rocks such as intrusive or sheared metamorphic rocks.

D: "Remobilized" grains (Figures 8C and 9), commonly referred to as flakes, are typically large but very flat grains, and thus, with a very small Corey factor. They can protrude from more bulky intergranular grains. They represent fracture filling in other minerals, silicate or sulfides, where gold has been remobilized by strain or hydrothermal processes. Extremely delicate, these grains are very sensitive to transport and promptly modified in sediments. Compared to other pristine classes, they are significantly less enriched in silver [56,75].

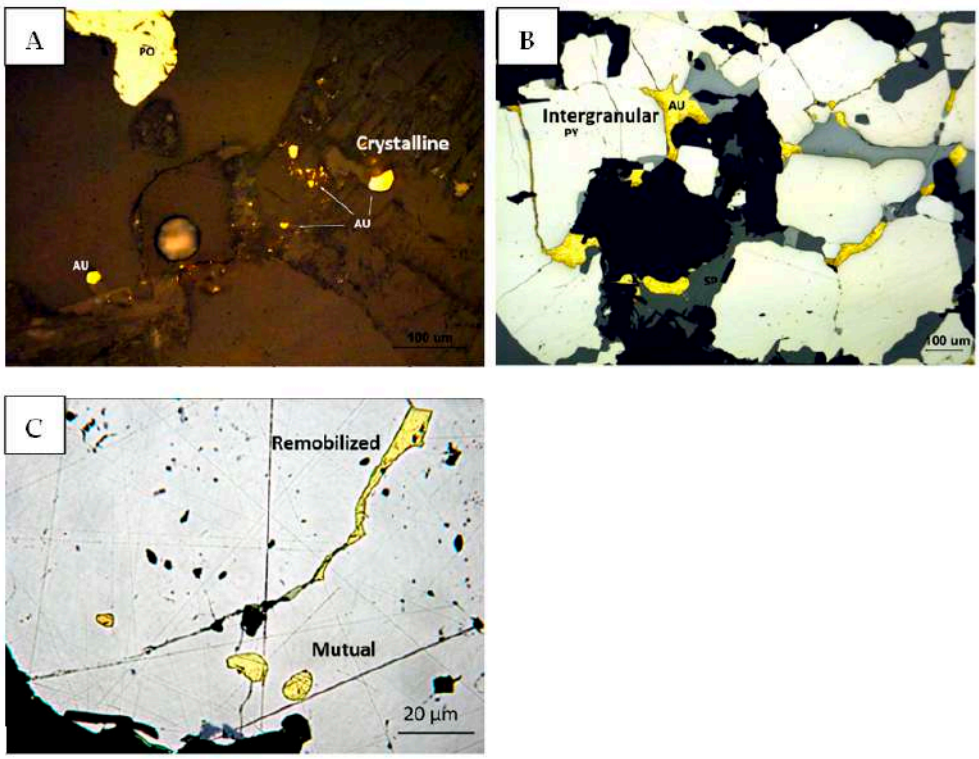

Figure 8. Examples of gold grain with the four main morphofacies as seen on a thin section with a petrographic microscope in reflected polarized light. (**A**) Crystalline grain in quartz. (**B**) Intergranular gold grain between pyrite, sphalerite and quartz. (**C**) Mutual gold droplet and remobilized leaflet in pyrite.

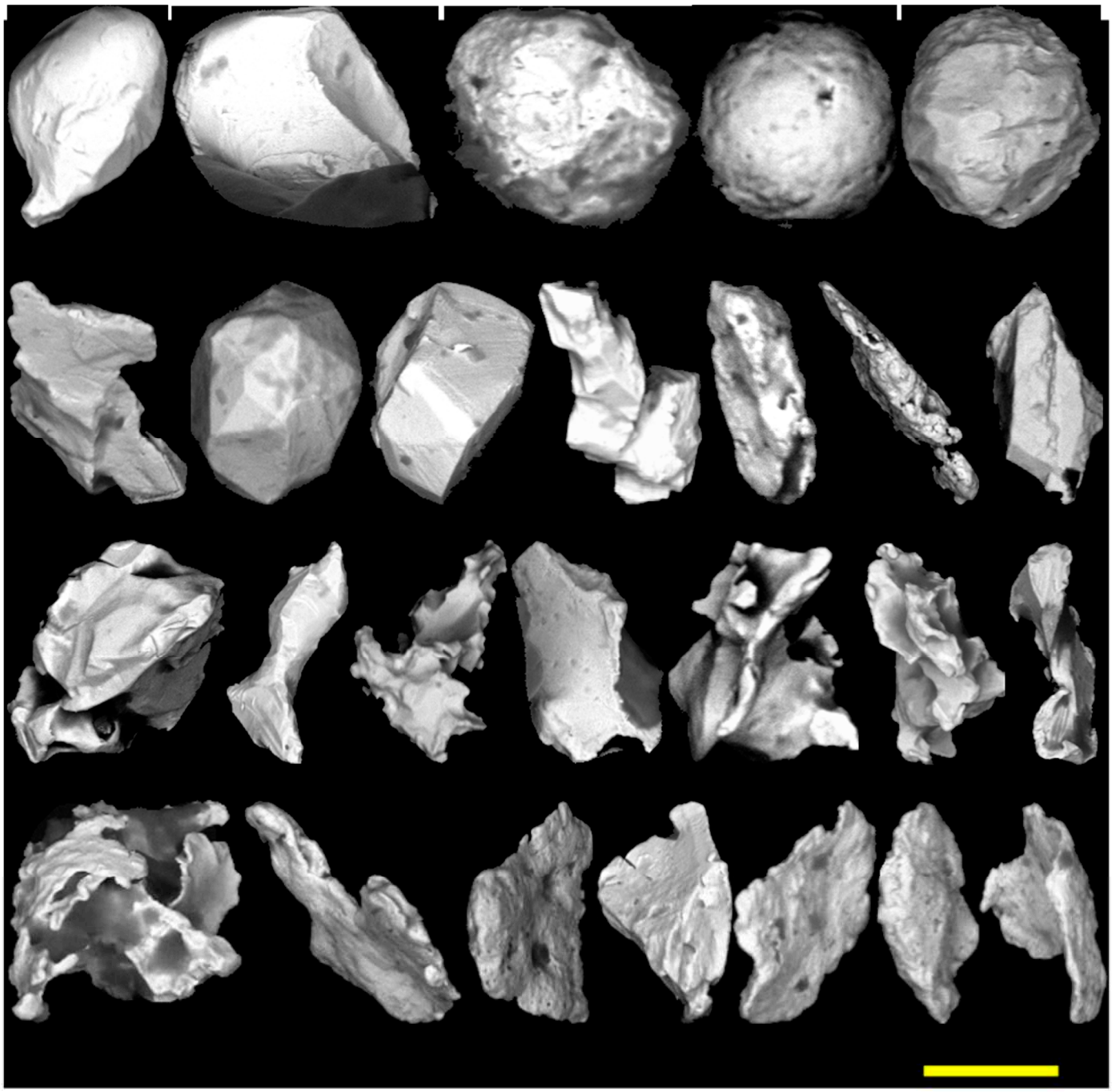

Figure 9. Mosaics of BSE images of grains classified as "mutual" (upper row), "crystalline," "intergranular" and "remobilized" (lower row). All images are BSE with a resolution 0.14 μm. Grains size range between 20 μm to 30 in μm length. Grains were selected from different samples and projects. Morphologies were classified with the used of ARTMorph automated CNN routine. Scale bar is approximately 20 μm in length.

Other unusual shapes, such as spherules [76], are occasional in sediments, but considered a curiosity.

Once again, these four morphofacies form a continuum of shapes. Although genuine shapes are easy to classify, intermediate forms can be difficult and easily misclassified by the mineralogist. For example, mutual bulbous shapes may evolve into crystalline by the presence of poorly developed facets, or intergranular grains may evolve into remobilized if they bear thin appendices. Furthermore, each of these shapes can be more or less affected by transport or dissolution, and thus, confused with modified shapes. The issue of these

continuums is partly addressed by the automated shape analysis. The grain image is deconvoluted in an array of mathematical parameters, which are then matched with the parameters of the truthing images. A quality of fit is calculated, yielding a probability of the match for each grain with the various classes. It has been demonstrated that Inception V.4 enables a better success rate at classifying images than human, as long as the system is properly trained [77]. The main advantage of such a system, aside from speed, is the reproducibility of the results, the same grain being always classified in the same class, as long as the system is based on the same training. Verification of class allocations from automated procedures made by a trained geologist suggests a misclassification rate of approximately 10%, a rate that is improving constantly with retraining of the system.

The grain size distribution of the different morphofacies is different (Figure 10), a phenomenon that can be induced partly by the intrinsic definition of the classes. Statistics on the populations are provided in Table 3. Mutual grains are distinctively smaller with a median of 17.9 µm, a size that is smaller than what can be efficiently identified with a stereomicroscope. By comparison, leafy "remobilized" grains are distinctively larger, with a median of 32.1 µm, almost twice the size of "mutual" grains. "Modified" and "reshaped" grains are still larger, and with a distribution distinctly skewed (asymmetry coefficient and kurtosis) toward large grains.

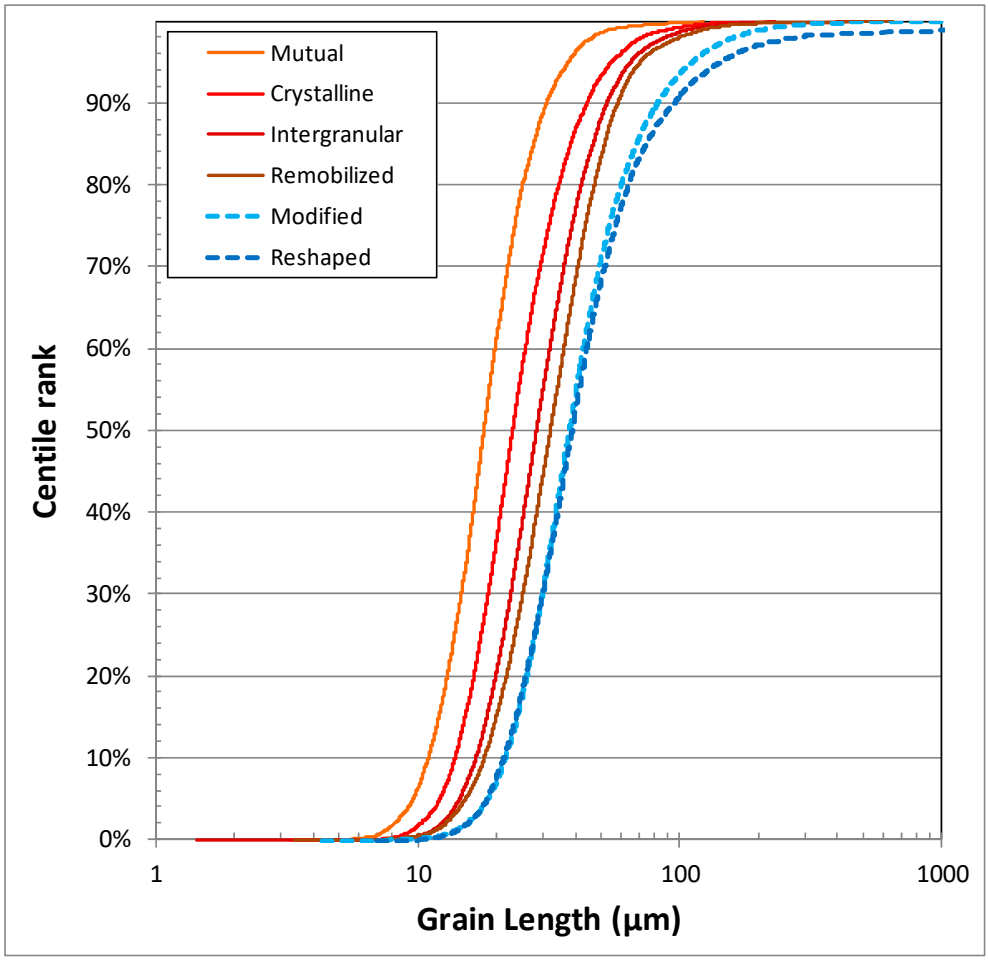

Figure 10. Size distribution of gold grains according to their shape. "Modified" and "Reshaped" grains are distinctively larger and skewed toward larger grains than the various type of "pristine," which themselves have different average size. "Reshaped" grains are twice the size, on average, of "mutual" grains, these being smaller than what can be measured with a stereomicroscope.

Table 3. Statistics of the size distribution of gold grains according to their shape. The variation in size (δmean) is the average size of a class, compared to the average size of the entire population. High asymmetry and Kurtosis are expected considering the log-normality of the distribution, but remain positive even when calculated on the logarithm of diameter. Axis ratio is the ratio of the width to length. Complexity is the ratio of the measured surface ($\pi ECD^2/4$) to the surface of the enclosing rectangle (L × l).

	Nb	Mean	δMean	Median	Std-Dev	Var.Co.	Asym.	Kurtosis	Axis Ratio	Complexity
Total	84,347	41.2	0%	31.5	61.8	1.5	17.6	410	0.68	0.71
Mutual	5198	20.0	−51%	17.9	10.0	0.5	2.9	17	0.72	0.75
Cryst.	8591	27.1	−34%	23.1	15.9	0.6	3.3	20	0.71	0.75
Interg.	21,406	33.0	−20%	28.4	20.2	0.6	4.9	57	0.66	0.68
Remob.	11,201	36.7	−11%	32.1	23.0	0.6	5.7	87	0.60	0.67
Modif.	27,775	48.3	17%	37.9	43.7	0.9	11.0	290	0.69	0.71
Reshap.	10,176	66.8	62%	38.9	152.8	2.3	8.4	77	0.73	0.75

Shapes can be characterized by a variety of parameters that can be extracted from the image by Aztec-Feature, or other image processing software such as Image-J 1.53d [78], Partisan [79]) or Zen 2.5-Pro (Carl Zeiss AG., Oberkechem, Germany). However, the surface of the grain being irregular with abundant shadows, some of these parameters, such as perimeter or rugosity, cannot be accurately measured by automated procedures. Only the maximum length and width were extracted from all grains, plus the area for 36,597 grains. The area is expressed as the equivalent circle diameter (ECD; $2\sqrt{S/\pi}$), which is the diameter of a circle with a surface equal to the measured area. From these, the axis ratio (l/L) quantifies the stubbiness or elongation of the grain, which ranges between 0.4 and 1 for most grains. The smallest average axis ratio is recorded for remobilized grains (0.6) while the maximum average is for reshaped grains (0.73), which is coherent with the abrasion that affected them (Table 3). Complexity is the ratio of the measured area to the enclosing rectangle $\pi ECD^2/(4 \times L \times l)$ and expresses how contorted the grain outline is. It scatters around that of an ellipse (0.78) for the vast majority of grains, but can be considerably lower for complex morphofacies such as "intergranular" or "remobilized." There is no strong relation between the axis ratio and complexity and these parameters are not efficient at discriminating morphofacies (Figure 11).

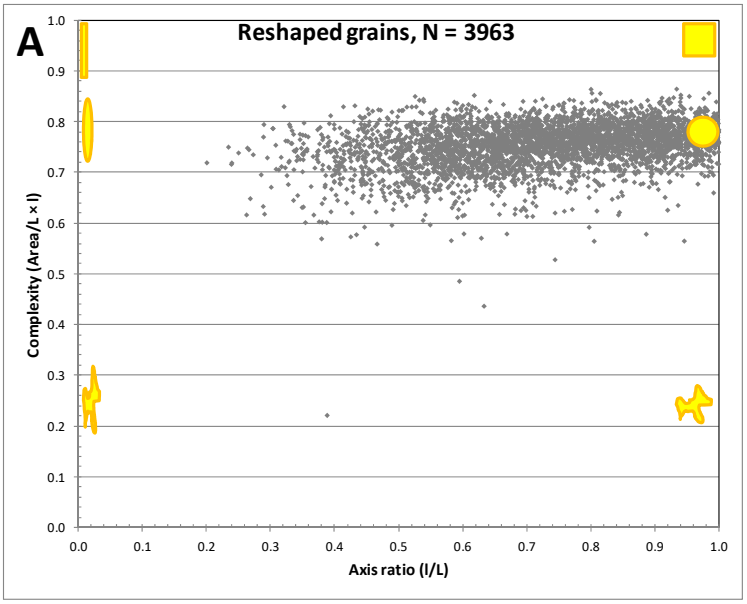

Figure 11. *Cont.*

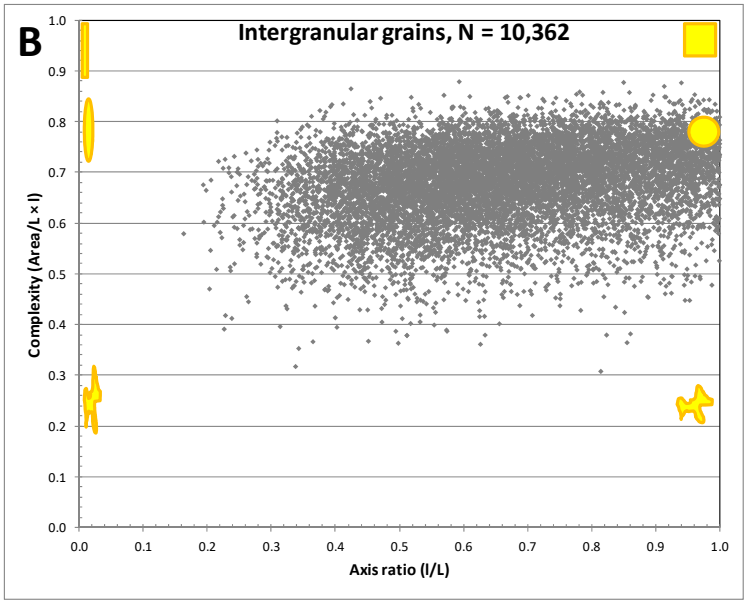

Figure 11. Relation between axis ratio and complexity for "intergranular" (**A**) and "reshaped" (**B**) grains. Other morphofacies are overlapping and intermediate between these two extremes. The axis ratio is the width divided by the length, and represents the stubbiness of the grains. The complexity is the ratio of the area, calculated from the ECD, divided by the area of the bounding rectangle (length × width). The smaller the ratio, the more contorted the shape, and an elliptical grain would have a complexity of 0.78. It is considered that the most "reshaped" grains were former "intergranular" grains that have been rounded in the course of sedimentary processes. Yellow forms are sketching the shape of grains with the corresponding axis ratio and complexity.

3. Discussion

The current dataset includes an accurate measurement of detrital gold grains size and morphology from a wide area over the Canadian Shield. All that is known about gold grain dispersion in the secondary environment has been based, until this study, on inaccurate visual estimates or on accurate data for very restricted areas. From these historic data, a variety of hypotheses were taken as granted by the exploration industry and seemed reasonable although not properly tested due to the lack of appropriate data. The current systematic measurements confirm or challenge a variety of these assumptions.

3.1. Similarity of Size Distribution

Gold grain size distributions obtained from various surveys are surprisingly similar, which phenomenon might be related to the log-normal distribution of grain size in source rocks. Lodgment tills from 16 geographically different projects, representing geologically unrelated environments, have a mean grain size between 31.6 µm and 43.9 µm. For example, the grain size distribution in a survey from the Opinaca sub-province, which consists of migmatitic terrain, is imperceptibly different from the distribution obtained in a survey conducted in the southern Abitibi sub-province, dominated by volcanics and related intrusions, almost 600 km away. The differences in the mean grain size from the various surveys are within one standard deviation of their distribution, and smaller than what can be measured without the help of an SEM.

Student t-tests (unilateral heteroscedatic) were computed for each pair of surveys to test if their average grain sizes on a logarithmic scale are significantly different despite their apparent similitude. Of the 120 pairs, 35 have *p*-values greater than 5%, meaning that there is an above-5% chance that both populations are not dissimilar. Inversely, 60 pairs have a *p*-value lesser than 0.1%, meaning that the similitude hypothesis is clearly rejected. However, considering how diverse and disjointed the surveys are, the tight overlap of the grain size distributions suggests that such a distribution is an intrinsic feature of orogenic-

related gold deposits. This observation, drawn from populations of grains originating from totally different geological environment, has numerous implications:

A: If a survey yields a grain size curve that is discrepant from the general trend, it likely means that the material is not a genuine till and that it underwent some sort of sedimentary sorting, and thus, cannot be considered as, and compared to, proper till surveys. The case has been experienced for surveys conducted by untrained samplers.

B: Similarly, if a survey yields a significantly coarser grain size distribution for samples that are genuine tills, it likely indicates that a recovery issue occurred in the laboratory and led to the loss of the finer grains. The conformity of the grain size distribution can, thus, be use as a powerful quality control test.

C: If a survey has been properly conducted and discrepancies are present in grain size distribution, it may mean that the gold grains were eroded from a radically different type of deposit, such as paleoplacers, skarn, Carlin type etc. Distinctive chemical signature or accessory mineral assemblages can be used to lessen the ambiguity.

D: Unless a survey encompasses drastically different geological provinces, such as a Paleozoic sequence on top of an Archean basement, or types of deposits, the sources of gold within the area are expected to have similar gold grain size distributions. As a result, the expected gold grain size distribution from a point source will be similar to the regional background, which combines multiple sources with similar grain size distribution. Consequently, it is very difficult to discriminate a dispersion train from the regional signal on the basis of the grain size distribution, unless detailed statistics on a sufficiently large population of grains are conducted.

This phenomenon is documented in the Borden area [13], where the gold grain size distribution curve of the samples collected down-ice of the mineralized zone have an apparently identical grain size distribution as those from the large regional survey (Figure 12). The Student t-test (bilateral, heteroscedatic) indicates a 12% chance that these two groups are not from dissimilar populations. Such difference is not significant and not discernible from basic statistics (mean, standard deviation etc.), nor is it from the cumulative plot.

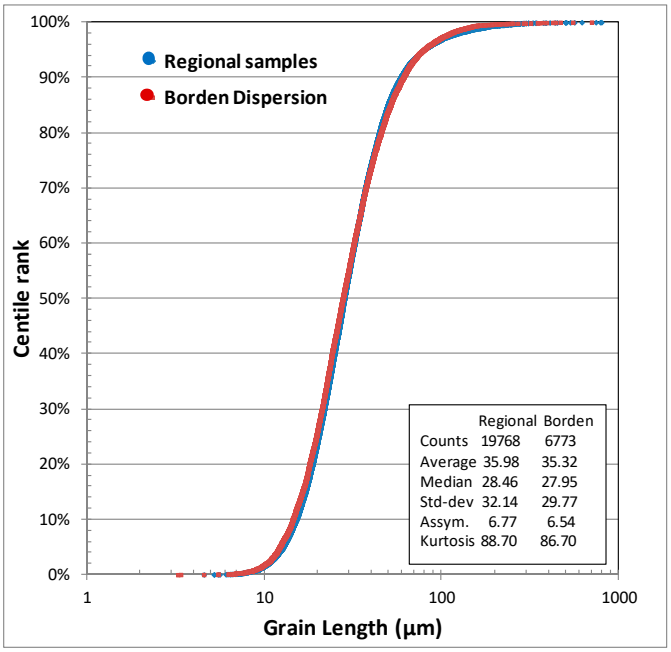

Figure 12. Cumulative size distribution curve of gold grain recovered from the dispersion train down-ice of Borden gold occurrence [13], versus the size distribution in the neighboring regional survey. Both populations are overlapping on the diagram, suggesting that fine gold grains are not dispersed further than the large one in the course of the glacial sedimentation process.

Hence, a Student t-test on grain size is recommended if one wants to test if a group of samples, suspected as representing a local dispersion train, is distinct from the regional signal.

3.2. Fine-Grained Gold Elutriation

It is commonly assumed that minute gold grains are easily washed away by the water flow. This assumption has been contradicted by two observations. Gold is extremely dense (17–19 g/cm^3), and sinks in water at a rate 2.14× faster than a silicate particle of the same size according to Stoke's law. A flow strong enough to wash away a gold grain 30 µm in diameter (median size) would also carry most silicate grains smaller than 64 µm. Therefore, the left-over material would be depleted of clay and silt. As seen in Figure 2, the clay-to-silt ratios of ablation or reworked tills are near identical to those of lodgment tills, meaning that preferential removal of clay-size material was limited and that fine-grained gold was likely not washed away in significant proportion. Moreover, the potentially washed-away gold grains would not have been sufficiently large to be recovered by the fluidized bed and not subjected to size and shape characterization. This has numerous implications in regard to mineral exploration:

A: The widespread concept that small grains in tills have traveled further than large ones, and thus are not representative of a local source, is a false and misleading assumption. This is exemplified by the Borden Gold dispersion trains (Figure 13), where samples close to the ore body have nearly identical grain size distributions to the samples a few kilometers down-ice. Consequently, the common belief that only large grains should be considered to be from local provenance is wrong, and using only these in the decision process is misguided.

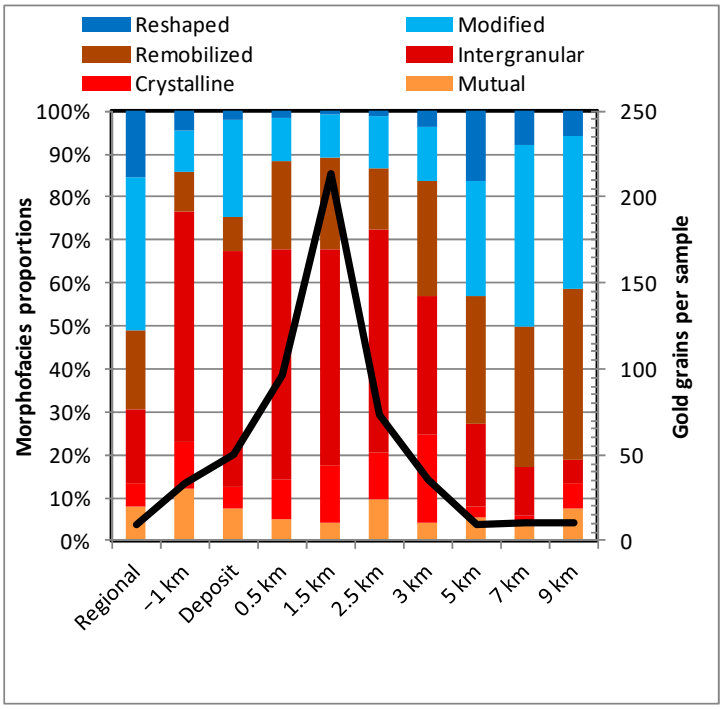

Figure 13. Relative proportions (% of grains) of each morphofacies (red hues are pristine, blues are modified or reshaped) down-ice of the Borden gold occurrence [13], as measured on the regional survey and along the various sampling fences of the orientation survey, starting 1 km up-ice from the deposit, on top of the deposit and along seven profiles located 0.5 to 9 km down-ice of the deposit. The average number of grains per samples for each profile is indicated by the black line (right scale). The regional samples contain 49% pristine grains, a typical proportion of most regional survey. This proportion sharply increases to 75–89% from slightly up-ice to 3 km down-ice of the deposit, to resume near to the regional level further south.

B: Ablation till, or even rework tills, have a similar gold grain size distribution (Figure 4), as well as a similar gold grain contents to lodgment tills [13]. This means that these did not lose their gold content, despite having been in contact with water. Thus, for the purpose of statistical analysis, both sets of samples can be merged into a single population. Care should be taken, however, in interpreting their distance of transport. It is a common belief that ablation tills are further traveled than lodgment till [80], an assertion that cannot be disproven with the current data. However, till samples down-ice from the Borden Gold deposit are both lodgment and ablation material, and no clear statistical difference is noted.

C: Small gold grains are not significantly washed away in the course of reverse circulation drilling (Figure 5), and this method seems adequate. However, screening or panning the material with water in the field is definitely not recommended, since it may lead to significantly small grain losses.

3.3. Morphology Changes with Transport

Gold being malleable, its shape is susceptible to be modified at the moment the grain is sheared or impacted. This phenomenon was tested by measuring the change of gold grain shape after milling, either in laboratory test or in mine concentrators. For example, grains recovered from a pilot plant lock-cycle on the ore from Cheechoo deposit (reduced felsic intrusion) were 63% pristine grains, 35% modified grains and 2% reshaped grains. Similar results were obtained from material out of the milling circuits of other operating mines (Figure 14). In most cases, the impact of milling on grain shape is limited, at least for grains with an average size of 20–30 μm. Thus, the process of milling the rock just enough to liberate the gold grains is not sufficient to significantly round or blunt the grains. The generation of reshaped grains seems to require a more protracted action or transport on the grains than what is usually experienced in a dispersion train rooted in a mineral occurrence.

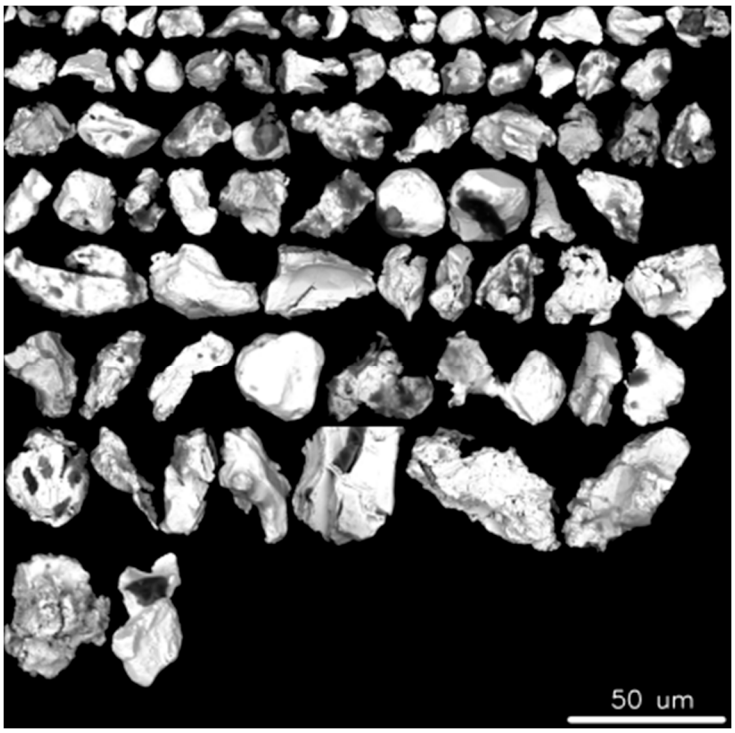

Figure 14. Mosaic of gold grains recovered from milling circuit of a mine concentrator. Notice that for the vast majority of grains, the initial shapes were not significantly modified by milling. Similar observations were made in materials from various mines located in the Abitibi, northern Québec.

Lodgment till is a rock gouge sheared at the base of the glacier and affected by minimal transport with little to no contact with water. It is expected to contain the grains least affected by deformation, considering their limited transport. Lodgment till samples contain an average of 59.7% pristine grains and 10.6% reshaped grains (Figure 15). Hybrid and ablation tills contain very similar proportions of the various shapes of grains as less-traveled lodgment tills. Just as for their counts and grain size distributions, shape proportions in lodgment and ablation tills are comparable and can be used indiscriminately. As expected, the proportion of modified and reshaped grains increases in reworked tills, and more drastically in alluvium and esker materials. A relation between rounding or blunting of gold grains and energetic or protracted water-borne transport is noted and seems required to produce rounded "reshaped" grains. The origin of the "reshaped" grains in tills, albeit less common (10%), is, therefore, up for debate.

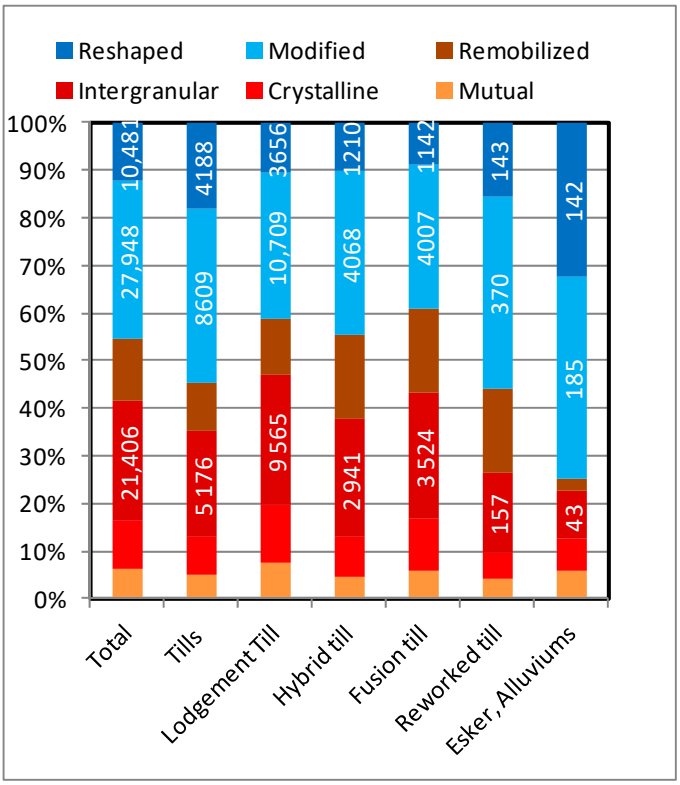

Figure 15. Proportion of the various morphofacies (reddish tints: pristine, blue: modified and reshaped) according to sediment types. Lodgment, hybrid and fusion tills have very similar proportions (58% pristine) while reworked tills, esker and alluviums show a drastic increase in more rounded grains (modified and reshaped), caused by attrition during water-borne transport. Undifferentiated tills are a poorly described material, and may include a variety of sediment types. Numbers indicated inside the bars are the grain counts of the specific class.

Assuming the regional background being even across the sampled area and neglecting the stochastic fluctuations [13], the presence of anomalous samples implies the contribution from a local source added to grains from the regional background. As the regional background contains a certain proportion of modified and reshaped grains, the addition of locally derived grains to the sample is likely to increase the abundance of pristine grains and barely contribute to the reshaped grain population. Consequently, samples with high counts are dominated by pristine grains. The proportion of grains of various shapes was computed for groups of samples with different grain counts (Figure 16). A steady increase in "pristine" grain abundance is noted with the overall grain abundance, from 29.5% in samples with less than 2 grains, to 86.8% in anomalous samples with more

than 256 grains. By comparison, "reshaped" grains decrease from 27.5% to 1.3%. This supports the hypothesis that samples with a few grains are essentially representing the regional background, which may varies from a few grains to a few tens of grains depending the area, and that grains added from a local source are vastly pristine and simply dilute the proportion of "modified" and "reshaped" grains from the background. It can also be noted that although the "pristine" grain abundance increases with counts, the proportion of "mutual" and "remobilized" grains is rather constant, and that the increase is mainly linked to addition of "intergranular" grains. The reason for this phenomenon is uncertain, but may originate from saturation of gold in the sulfides of the source material, leading to a maximum abundance of "mutual" grains, while the excess gold precipitate later at the grain boundaries.

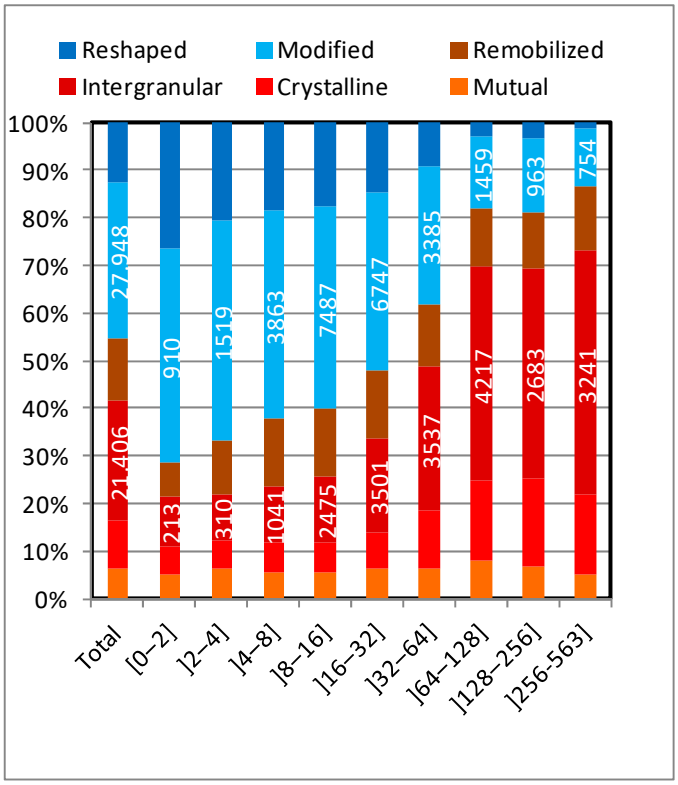

Figure 16. Proportion of the various morphofacies (reddish tints: pristine, blue: modified and reshaped) according to grain abundance in the samples. A steady increase in pristine grain abundance is noted, from 29.5% in samples with 2 or fewer grains, to 86.8% in highly anomalous samples. This suggests that "modified" and "reshaped" grains are dominantly contributed by the regional background, and are diluted by pristine grains derived from a local source. Numbers indicated inside the bars are the grain counts of the specific class.

There are a few cases in the northeastern Abitibi sub-province where the samples with elevated counts include abnormally abundant "modified" or "reshaped" grains. Such an anomaly suggests that the till incorporated recycled sediments that were lying on top of the basement prior to glaciation, such as what happen where multiple glacial drift direction are recorded [81]. Although such deposits can be genuine lodgment tills, they may incorporate older, gold-bearing, non-glacial sediments. The ambiguity can then be lifted by comparing the gold grain size distribution of the samples with the general distribution indicated in Figure 4, which shows that recycled sediments have a discrepantly coarser distribution.

A relation between the shape and transport distance is commonly invoked in mineral exploration. It has even been suggested [1,36] that the transport distance can be estimated from the shape of a grain, with "pristine" grains being less than 100 meters from the source and the source of "reshaped" grains being more than a kilometer away. No indications were

provided as to how the ice dynamic and velocity influence these distances, which were provided as guidelines for mineral exploration. Such a hypothesis can be tested using a dispersion train with detailed sampling, as was done for the Borden Gold survey [13]. This deposit, approximately 1 kilometer in length, is orthogonal to the ice flow direction and the source of an intense dispersion trains. A vast regional survey (935 samples) encompasses the area up-ice of the deposit, providing an accurate measurement of the background signal incoming toward the deposit. The background signal is calculated at 9.1 grains per sample, with 49% "pristine," 36% "modified" and 11% "Reshaped" grains. A series of seven sampling profiles is available, starting 1 kilometer up-ice of the deposit, then atop the deposit, then from 0.5 km to 9 kilometers down-ice. Grain abundances 1 kilometer up-ice of the deposit are anomalous with an average of 33 grains, a phenomenon interpreted as the erosion of the mineralized halo of the deposit. Counts increase exponentially up to 214 grains per samples at 1.5 kilometer down-ice. They then decrease progressively until background abundance is recorded 5 km down-ice of the deposit. Similarly, the abundance of "pristine" grains increases along with the abundance of grains, oscillating between 75% and 89% in the various profiles as far as 3 km down-ice. It then drops to near background values of 50–58% "pristine" grains. The contribution of the deposit is, therefore, obvious from −1 km to 3 km down-ice, indicating a >4 km long dispersal train. Further down-ice, only a slight increase in "pristine" grain proportion is noted compared to background signal, which can be confused with the natural variance of the samples. The abundance of "reshaped" grains across the various profiles is not related to the overall grain abundance, ranging between 0.6 to 1.54 grains per sample, or 0.5% at the peak of the anomaly compared to 15% in the regional background. This suggests that erosion of the deposit did not contribute to their abundance. As "reshaped" grains originate only from the diluted regional signal and did not increased along the dispersion train, it cannot be concluded that rounding and blunting of grains is directly related to the distance of glacial transport. Assigning a transport distance to a specific morphofacies, or estimating this distance from the mere abundance of pristine grain can, thus, be misleading. The only definitive conclusion is that abundant pristine are typically indicative of a local source. However, a detailed account of these proportions cannot be translated into absolute transport distance.

The ominous mixture of deformed and pristine grains in the same samples raises questions on how grains are deformed and why some are preserved. A simple stochastic process is considered unlikely, and the rate of deformation is likely a function of the original shapes. Examining the BSE images of a multitude of grains suggests that fragile shapes, such as delicate remobilized flakes, are easier to blunt than stubby crystalline grains. Thus, these remobilized flakes are promptly morphed into "modified" or even "reshaped" grains and their chances of surviving shearing or attrition is low. Similarly, intergranular grains typically have stubby outlines, but with very delicate edges. Thus, upon shearing or attrition, the general outline would be preserved, but the edges would promptly be blunted, as is observed. "Intergranular" grains are labeled as such when the original shape is discernible. However, a complete continuum is noted with "modified" grains, and it seems that the bulk of these "modified" grains are former "intergranular" grains. A very similar phenomenon is observed for "crystalline" grains, although intense deformation is noticeable only on the large polycrystalline dendrites. "Mutual" grains, being initially rounded, are less susceptible to be deformed and difficult to discriminate from "reshaped" ones when small.

A relation exists between proportions of "pristine" or "deformed" grains and grain size (Figure 17). At 10 μm or less, about 92% of the grains are "pristine," compared to none of the grains larger than 1 mm. The 20–30 μm group, the most abundant group encompassing the median grains, has 60% "pristine" grains. Inversely to "pristine" grains, the abundance of "reshaped" grains increases progressively, more markedly for grains larger than 150 μm. This increase in deformation with size is explained by the higher probabilities of small grains eluding impact or shear because they are more easily liberated

than large contorted grains, they are more susceptible to be hidden in anfractuosities of larger ones, they can escape local stress field by sliding between other grains and they have higher resistance due to their stubbiness. Inversely, large grains are typically more contorted with complex edges and appendices that can be easily blunt, are more likely to be anchored between other grains in the source rocks and are more exposed to shearing or impact.

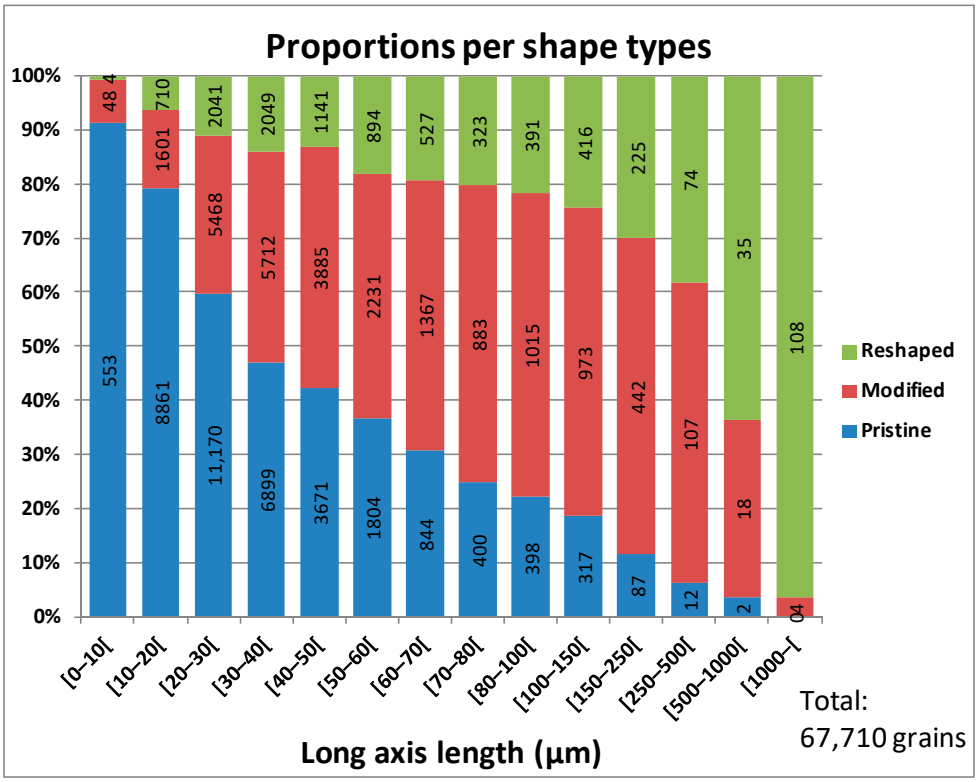

Figure 17. Proportions of "pristine," "modified" and "reshaped" grains in till according to their size. The diagram is based on a subset of 67,710 grains, all classified from BSE images using the same version of ARTMorph routine. The constant decrease in "pristine" grain abundance with size is stark, ranging from 92% in grains smaller than 10 µm, to 0% for grains larger than 1 mm. Note that the scale axis is linear up to 100 µm, after which it becomes approximately logarithmic. At the typical median size of 20–30 µm, approximately 60% or the grains are "pristine," which is close to the overall average of the database.

Based on the aforementioned factors, the abundance of "pristine" grains is a more complicated issue than usually considered, and interpreting the proximity of the source material should be done with care. The presence of large but delicate "remobilized" grains is a clear indication of proximity, while small stubby "mutual" grains can travel almost indefinitely. Thus, the abundance of "pristine" grains should be weighted for their size and morphology while interpreting the surveys and prioritizing exploration targets. However, how influential these are on a statistical basis has not been tested yet, and it is possible that such effects are marginal considering that the bulk of "pristine" grains are "intergranular" and the bulk of these grains are in the 20–50 µm range. If grains are sufficiently abundant, it might be suitable to use only the abundance of "intergranular" grains on count maps to select anomalies. As seen on Figure 13, in the Borden dispersion train, "intergranular" grains are amply sufficient to outline the dispersion and offer the highest anomaly versus background counts, or signal-to-noise ratio.

Another process that is invoked for the presence of pristine grains far from their source is that grains are deformed only once they are liberated, and that liberation may

occur down-ice from the source rock. Otherwise said, they may have been transported encapsulated in a polymineralic particle that has subsequently been disaggregated. Based on what is observed in gold deportment studies for material from mills and concentrator, gold grains are easily liberated and only a minute proportion of the grains remains attached to other minerals. Similarly, in tills, only a tiny fraction (<0.5% estimated) of grains shows such attachment. Heterogeneities in a particle tend to focalize the internal stress field, leading to breakage. Since gold is malleable compared to host minerals, the stress field applied to a particle is concentrated on gold grains, leading to preferential breakage of the particle where the gold grain is, especially if this grain is located at the gangue mineral interface. Then, the grain is liberated. It has been observed by the authors that to remain encapsulated in a particle in course of milling, a gold grain needs to be less than one-tenth of the particle diameter. Such small gold grains encapsulated in sulfides or silicates would not increase the density of the particle enough to enable its recovery by gravity methods, and such particles will not be recovered and counted. Consequently, no evidence of the process is noted in glacial sediments.

Another question is how much of the fine material in the till is derived from attrition of the coarser particles and fragments (pebbles, boulders, etc.) in the course of transport, compared to the fine material released from the direct erosion of the bedrock and whether it is sufficient to contribute significantly to the gold grain abundance. The only available clue is the diminution in the abundance of clasts and the volume of material that has been abraded from sub-angular pebbles in ablation tills, compared to angular clasts in the lodgment till. Such a proportion is estimated as small, and not enough to account for the proportion of pristine grains in such sediments.

The issue of oxidation of sulfide is also commonly invoked to explain the presence of pristine gold grains away from their source rock. Since gold has a tendency to associate with sulfides, it can, thus, be attached or encapsulated within sulfide particles which are resistant to mechanical breakage. Heavy mineral studies using automated mineral counting indicated that sulfides are far less abundant in glacial sediments than in source rocks, even in sediments that have no evidence of oxidation. This sulfide deficiency is noted for lodgment tills, which do show evidence of oxidizing water, and is dramatic in the ablation or reworked tills, in which there is an almost complete absence of sulfides. Abundance of sulfides has been observed only in lodgment tills sampled by drilling in thick overburden sequences, such as underneath the Ojibway glaciolacustrine clays. If originating from sulfide dissolution, the relative abundance of pristine grains in tills (average of 50% of grains) would require that an unrealistic proportion of the gold would need to be associated with sulfides, while gold tends to be mechanically liberated during basement erosion. Still, the process remains a reasonable explanation to the presence of isolated and non-replicable high counts, which could not be related to local sources but to the possible oxidation and disaggregation of a sulfide-rich boulder.

3.4. Meaning of the Different Pristine Morphofacies

The shape classification scheme for "pristine" gold grains has been elaborated early in the development of the procedure and is based on examination of the BSE high resolution images. The initial observation was that grains can record the imprints of surrounding minerals. From then, the four morphofacies classification scheme based on what the shape of the grain may suggest as crystallization environment has been developed. No detailed studies, such as one using microtomography, were conducted on how such shapes may relate to in situ gold grains. Thus, the classification is still embryonic. If the classification is assumed as sound, conclusions can be drawn from the grain shapes in regard to the source rocks and used for mineral exploration decision.

When a detrital gold anomaly is located in the till, the next exploration step is usually not to conduct a supplementary closely spaced till sampling because the spatial resolution of the method ranges from a few hundred meters to a kilometer. Thus, if basic outcrop prospecting fails to locate the source rock, other indirect exploration methods with better

spatial resolution is required, such as soil geochemistry or geophysics. The dominant factor that would determine the response of the mineralization to either geochemistry or geophysics is the presence, or absence, of associated sulfides. Gold is associated with sulfides, dominantly pyrite, chalcopyrite and arsenopyrite, in most orogenic deposit, but not all of them. For example, in reduced intrusion-related gold system, gold can be disseminated in barely mineralized rocks with less than 1% total sulfides [82]. The abundance of sulfides, which are conductive to electricity, will dictate the geophysics responses of the rocks. Sulfide-rich rocks will be conductive, rock disseminated with sulfides will be chargeable and barren rocks will be resistive. The presence of gold grains the shape of which may suggest their association with sulfides, such as the rounded "mutual" grains, will provide insights on which type of geophysical response should be expected. Inversely, gold grains with shapes that may suggest growth in a sulfide-free environment, such as the "crystalline" grains that are suspected to have grown in quartz or carbonate veins, will not respond to induced polarization, and would tend to be associated with resistivity anomalies. Similarly, sulfidic zones tend to oxidized when in contact to groundwater, which then create a galvanoplastic cell driving metal cations to surface [83]. This process is known as releasing the metal charge from the source rock, which migrates to the surface, to precipitate or accumulate as hydromorphic geochemical anomalies. Inversely, sulfide-free gold mineralization, such as quartz-veins systems, will not tend to weather and and release its metal content to the secondary environment; moreover, it will not cause contrasting geochemical anomalies. Thus, the insights provided by the shape of gold grains, either suggesting a sulfidic or sulfide-free source rock, shall be of help in follow-up geochemistry survey. Further testing is needed in regard to these working hypotheses.

4. Conclusions

Gold grain is the best indicator mineral to be used in drift prospecting for gold deposits. Automated high resolution backscattered electron imaging of the grains enables accurate size and shape measurements that can be used to assess the validity of some exploration precepts or to provide insights for exploration decisions.

- Grain size distribution approximately follows a log-normal distribution that is bounded by the instrumental limitations at 1 mm due to sieving and approximately 10 µm due to recovery limitations. This grain size distribution is relatively constant between surveys, areas and deposits. Discrimination of grains from dispersion train versus background signal requires detailed statistical analysis such as Student tests. However, it can efficiently be used without advanced statistics to detect sampling or processing issues.
- Gold grain size distribution obtained in lodgment tills is similar to size distribution in source rocks if such a material is process with the same laboratory procedure.
- No significant difference is noted between gold grain size distribution from various types of glacial sediments, except for high energy alluvial or beach sediments. It suggests that gold grain elutriation by natural processes occurs only at sizes smaller than what can be recovered by heavy mineral concentration procedures. Ablation and lodgment tills from an area constitute a uniform population in this regard and do not require separated statistical interpretations. No significant fine-grained gold loss is noted for samples collected by reverse circulation drilling.
- Gold grain shape is dictated by their relation with neighboring minerals in the source rock, which is rather well preserved by erosion and transport. Four morphofacies are here introduced: "Mutual" grains that are rounded droplet typically found in sulfides; "Crystalline" grains that have at the least partially developed the cubic crystalline habits and considered as originating dominantly from unconstrained growth in quartz or carbonates; "Intergranular" grains with complex shapes, which are dictated by neighboring minerals boundaries; and "remobilized" grains that are leaflets and flakes

that filled cracks in other minerals. These four morphofacies are subdivisions of the pristine class.

- No significant difference is noted in grain morphofacies abundance between the various type of sediments, except for reworked till, alluvial sediments and beach sediments, where "reshaped" grains are more abundant.
- The relative morphofacies abundance can be used to forecast the association of gold with sulfides and orient geophysical survey and interpretation.
- The rate at which the shape of the grain is modified in the course of sediment transport is dependent on the size of the grain, small grains being less susceptible to deformation. It is also dependent on shape complexity, delicate grains such as remobilized leaflets being more readily modified than rounded mutual grains. This implies that estimation of the transport distance cannot be simply based on the "pristine" to "Modified plus reshaped" grains without taking into account the initial size and shape of the grains. Drawing exploration conclusions on such premises can be misleading.
- Regional gold grain backgrounds typically have a 50–30–20 ratio between "pristine," "modified" and "reshaped" grains. The presence of a dispersion trains eroded from a local source will typically contribute dominantly to the "intergranular-pristine" grain population, without significant contribution to "reshaped" population. If counts are sufficient to circumvent the intrinsic variance induced by the Poisson distribution, the count of "intergranular" grains provides the best signal-to-noise ratio for interpreting the results.

Supplementary Materials: The following are available online at https://www.mdpi.com/article/10.3390/min11040379/s1, Table S1: Gold grain measurement, shape and semiquantitative EDS analyses.

Author Contributions: Conceptualization, R.G.; validation, H.L.; formal analysis, R.G.; investigation, R.G. and S.M.; writing (original draft preparation), R.G.; writing (review and editing), H.L.; project administration, R.G.; funding acquisition, None; Data Acquisition, J.T.; Computer and programming, A.N. All authors have read and agreed to the published version of the manuscript.

Funding: All contributions to this project is from IOS Services Géoscientifiques Inc.

Data Availability Statement: The data presented in this study, excluding the provenance of the samples, are available on request from the corresponding author. The data are not publicly available being of sensitive nature in regard of mineral exploration issues that are confidential to the author's clients.

Acknowledgments: Goldcorp Corporation is acknowledged for granting permission to initially publish the data acquired on their property and used for Figure 13. Patrice Villeneuve, Phillipe Pagé, Marie-Odile Chartier, Natacha Fournier, Karen Gagné and Mélanie Aubin (IOS Services Géoscientifiques Inc.) are thanked for their valuable assistance with quaternary geology, SEM work, database management and map design, respectively. The anonymous reviewers are thanked for their constructive comments that improved the manuscript considerably. The editors are thanked for their careful editorial handling.

Conflicts of Interest: R.G. is the general manager of IOS Services Géoscientifiques Inc., and participated in the development and commercialization of the analytical method used to acquire the data assessed in this study.

References

1. Averill, S.A.; Zimmerman, J.R. The riddle resolved—The discovery of the Partridge Gold Zone using sonic drilling in glacial overburden at Waddy Lake, Saskatchewan. In *CIM Bulletin*; Canadian Institute of Mining, Metallurgy and Petroleum: Westmount, QC, Canada, 1984; Volume 77, p. 88.
2. Sarala, P.; Pulkkinen, E.; Ojala, V.J.; Peltoniemi-Taivalkoski, A. Gold exploration using till at Petäjälehto, northern Finland. *Geochem. Explor. Environ. Anal.* **2009**, *9*, 247–255. [CrossRef]
3. McClenaghan, M.B.; Cabri, L.J. Review of gold and platinum group element (PGE) indicator minerals methods for surficial sediment sampling. *Geochem. Explor. Environ. Anal.* **2011**, *11*, 251–263. [CrossRef]

4. Averill, S.A. Discovery and delineation of the rainy river gold deposit using glacially dispersed gold grains sampled by deep overburden drilling: A 20-year odyssey. In *New Frontiers for Exploration in Glaciated Terrain*; Paulen, R.C., McClenaghan, M.B., Eds.; Open File 7374; Geological Survey of Canada: Ottawa, ON, Canada, 2013; pp. 37–46.
5. Taivalkoski, A.; Sarala, P.; Hulkki, H. Gold exploration using heavy minerals in till and weathered bedrock in Petäjäselkä, northern Finland. *Geochem. Explor. Environ. Anal.* **2015**, *15*, 205–221. [CrossRef]
6. Dilabio, R.N.W. Classification and interpretation of the shapes and surface textures of gold grains from till. In *Gisements Alluviaux d'or (Alluvial Gold Placers/Yacimientos Aluviales de Oro)*; Geological Survey of Canada Contribution N 32391; ORSTOM: Paris, France, 1991; pp. 297–313.
7. Harris, D.C. The mineralogy of gold and its relevance to gold recoveries. *Miner. Depos.* **1990**, *25*, S3–S7. [CrossRef]
8. Haycock, H.M. The role of the microscope in the study of gold ores. *Can. Inst. Min. Metall.* **1937**, *40*, 405–414.
9. Sauerbrei, J.A.; Pattison, E.F.; Averill, S.A. Till sampling in the Casa-Berardi gold area, Quebec: A case history in orientation and discovery. *J. Geochem. Explor.* **1987**, *28*, 297–394. [CrossRef]
10. Averill, S.A. Regional variations in the gold content of till in Canada. In *Prospecting in Areas of Glaciated Terrain*; MacDonald, D.R., Mills, K.A., Eds.; Canadian Institute of Mining and Metallurgy: Montréal, QC, Canada, 1988; pp. 271–284.
11. Huhta, P. Studies of till and heavy minerals for gold prospecting at Ilomantsi, eastern Finland. In *Prospecting in Areas of Glaciated Terrain*; MacDonald, D.R., Mills, K.A., Eds.; Canadian Institute of Mining and Metallurgy: Montréal, QC, Canada, 1988; pp. 285–292.
12. Huhta, P. The use of heavy mineral concentrates from till in gold exploration in the late Archean Hattu Schist belt, Ilomantsi, Eastern Finland. *Geol. Surv. Finl.* **1993**, *17*, 363–372.
13. Girard, R.; Tremblay, J.; Néron, A.; Longuépée, H. Automated gold grain counting. Part 1: Why counts matter! *Minerals* **2021**, *11*, 337. [CrossRef]
14. Boivin, J.-F.; Bédard, L.P.; Longuépée, H. Counting a pot of gold: A till golden standard. *J. Geochem. Explor.* **2021**. submitted.
15. McClenaghan, M.B. Regional and local-scale gold grain and till geochemical signatures in the Western Abitibi greenstone Belt, central Canada. In *Drift Exploration in Glaciated Terrain*; Special Publication 185; McClaneagan, M.B., Bobrowsky, P.T., Hall, G.E.M., Cook, S.J., Eds.; Geological Society: London, UK, 2001; pp. 201–223.
16. Sciuba, M.; Beaudoin, G.; Grzela, D.; Makvandi, S. Trace element composition of scheelite in orogenic gold deposits. *Econ. Geol.* **2020**, *55*, 1149–1172. [CrossRef]
17. Sciuba, M.; Beaudoin, G.; Makvandi, S. Chemical composition of tourmaline in orogenic gold deposits. *Econ. Geol.* **2020**. [CrossRef]
18. Averill, S.A. Indicator minerals fingerprinting in surficial sediments near Au-Cu deposits of the porphyry-epithermal-volcanogenic suite. In Proceedings of the 26th International Applied Geochemistry Symposium, Rotorua, New Zealand, 17–21 November 2013; pp. 35–44.
19. Hashmi, S.; Ward, B.C.; Plouffe, A.; Leybourne, M.; Ferbey, T. Geochemical and mineralogical dispersal in till from the Mount Polley Cu-Au porphyry deposit, central British Columbia, Canada. *Geochem. Explor. Environ. Anal.* **2015**, *15*, 234–249. [CrossRef]
20. Plouffe, A.; Ferbey, T.; Hashmi, S.; Ward, B.C. Till geochemistry and mineralogy: Vectoring towards Cu porphyry deposits in British Columbia, Canada. *Geochem. Explor. Environ. Anal.* **2016**, *16*, 213–232. [CrossRef]
21. Plouffe, A.; Ferbey, T. Porphyry Cu indicator minerals in till: A method to discover buried mineralization. In *Indicator Minerals in Till and Stream Sediments of the Canadian Cordillera*; Ferbey, T., Plouffe, A., Hickin, A.S., Eds.; Geological Association of Canada: Ottawa, ON, Canada, 2017; Volume 50, pp. 129–159.
22. Clark, J.R.; Williams-Jones, E.W. Rutile as a potential indicator mineral for metamorphosed metallic ore deposits. *Divex Final Rep. Sub Proj. SC2* **2004**. 17 pages.
23. Dupuis, C.; Beaudoin, G. Discriminant diagrams for iron oxide trace element fingerprinting of mineral deposit types. *Miner. Deposita.* **2011**, *46*, 319–335. [CrossRef]
24. Dare, S.A.S.; Barnes, S.J.; Méric, J.; Néron, A.; Beaudoin, G.; Boutroy, E. The use of trace elements in Fe-oxides as provenance and petrogenetic indicators in magmatic and hydrothermal environments. In Proceedings of the 12th SGA Biennial Meeting, Uppsala, Sweden, 12–15 August 2013; Volume 1, pp. 256–259.
25. Huang, X.-W.; Boutroy, E.; Makvandi, S.; Beaudoin, G.; Corriveau, L.; Franco De Toni, A. Trace element composition of iron oxides from IOCG and IOA deposits: Relationship to hydrothermal alteration and deposit subtypes. *Miner. Depos.* **2019**, *54*, 525–552. [CrossRef]
26. Huang, X.-W.; Sappin, A.A.; Boutroy, E.; Beaudoin, G.; Makvandi, S. Trace element composition of igneous and hydro-thermal magnetite from porphyry deposits: Relationship to deposit subtypes and magmatic affinity. *Econ. Geol.* **2019**, *114*, 917–952. [CrossRef]
27. Makvandi, S.; Huang, X.W.; Beaudoin, G.; Quirt, D.; Ledru, P.; Fayek, M. Trace element signatures in hematite and goethite from Kiggavik-Andrew Lake Structural Trend uranium deposits and prospects (Nunavut, Canada). *Miner. Depos.* **2020**, *56*, 509–535. [CrossRef]
28. Nadoll, P.; Angerer, T.; Mauk, J.L.; French, D.; Walshe, J. The chemistry of hydrothermal magnetite: A review. *Ore Geol. Rev.* **2014**, *61*, 1–32. [CrossRef]
29. McClenaghan, M.B.; Parkhill, M.A.; Pronk, A.G.; Sinclair, W.D. Indicator mineral and till geochemical signatures of the Mount Pleasant W-Mo-Bi and Sn-Zn-In deposits, New Brunswick, Canada. *J. Geochem. Explor.* **2017**, *172*, 151–166. [CrossRef]

30. McClenaghan, M.B. Indicator mineral methods in mineral exploration. *Geochem. Explor. Environ. Anal.* **2005**, *5*, 233–245. [CrossRef]
31. Hooke, R.L.B.; Cummings, D.I.; Lesemann, J.-E.; Sharpe, D.R. Genesis of dispersal plumes in till. *Can. J. Earth Sci.* **2013**, *50*, 847–855. [CrossRef]
32. Griffin, W.L.; Ryan, C.G. Trace elements in indicator minerals: Area selection and target evaluation in diamond exploration. *J. Geochem. Explor.* **1995**, *53*, 311–337. [CrossRef]
33. McClenaghan, M.B.; Kjarsgaard, B.A. Indicator mineral and geochemical methods for diamond exploration in glaciated terrain in Canada. In *Drift Exploration in Glaciated Terrain*; McClenaghan, M.B., Bobrowsky, P.T., Hall, G.E.M., Cook, S.J., Eds.; Geological Society: London, UK, 2001; Volume 185, pp. 83–123.
34. Malkovets, V.G.; Rezvukhin, D.I.; Belousova, E.A.; Griffin, W.L.; Sharygin, I.S.; Tretiakova, I.G.; Gibsher, A.A.; O'Reilly, S.Y.; Kuzmin, D.V.; Litasov, K.D.; et al. Cr-rich rutile: A powerful tool for diamond exploration. *Lithos* **2016**, *265*, 304–311. [CrossRef]
35. Makvandi, S.; Pagé, P.; Tremblay, J.; Girard, R. Exploration for platinum-group minerals in till: A new approach to recovery, counting, mineral identification and chemical characterization. *Minerals* **2021**, *11*, 264. [CrossRef]
36. McClenaghan, M.B.; Paulen, R.G.; Oviatt, N.M. Geometry of indicator mineral and till geochemistry dispersal fans from the Pine Point Mississippi Valley-type Pb-Zn district, Northwest Territories. *Can. J. Geochem. Explor.* **2018**, *190*, 69–86. [CrossRef]
37. Giusti, L. The morphology, mineralogy, and behavior of "fine-grained" gold from placer deposits of Alberta: Sampling and implications for mineral exploration. *Can. J. Earth Sci.* **1986**, *23*, 1662–1672. [CrossRef]
38. Bernier, M.A.; Webber, G.R. Mineralogical and geochemical analysis of shallow overburden as an aid to gold exploration in southwestern Gaspésie, Quebec, Canada. *J. Geochem. Explor.* **1989**, *34*, 115–145. [CrossRef]
39. Nikkarinen, M. Size, form and composition of gold grains in glacial drift in Ilomantsi, eastern Finland. *J. Geochem. Explor.* **1991**, *39*, 295–302. [CrossRef]
40. Saarnisto, M.; Tamminen, E.; Vaasjoki, M. Gold in bedrock and glacial deposits in the Ivalojoki area, Finnish Lapland. *J. Geochem. Explor.* **1991**, *39*, 303–322. [CrossRef]
41. Nikolaeva, L.A.; Nekrasova, A.N.; Milyaev, S.A.; Yablokova, S.V.; Gavrilov, A.M. Geochemistry of native gold from deposits of various types. *Geol. Ore. Deposit.* **2013**, *55*, 176–184. [CrossRef]
42. Grant, A.H.; Lavin, O.P.; Nichol, I. The morphology and chemistry of transported gold grains as an exploration tool. *J. Geochem. Explor.* **1991**, *40*, 73–94. [CrossRef]
43. Nichol, I.; Lavin, O.P.; McClenaghan, M.B.; Stanley, C.R. The optimization of geochemical exploration for gold using glacial till. *Explor. Min. Geol.* **1992**, *1*, 305–326.
44. Goldfarb, R.J.; Groves, D.I. Orogenic gold: Common or evolving fluid and metal sources through time. *Lithos* **2015**, *233*, 2–26. [CrossRef]
45. McQueen, K.G.; Bielin, S.; Lennie, C.A. *The Nature of Pyritic Gold Ores at Kalgoorlie, Western Australia: Geological and Metallurgical Implications*; James Cook University of North Queensland, Contributions of the Economic Geology Research Unit 51: Townsville, Australia, 1994; p. 42.
46. Liu, H.; Beaudoin, G.; Makvandi, S.; Jackson, S.E. Geochemical signature of native gold from various Au- bearing deposits -implications for mineral exploration. In Proceedings of the 15th SGA Biennial Meeting, Glasgow, Scotland, UK, 27–30 August 2019; pp. 675–678.
47. DiLabio, R.N.W. Gold abundances vs. grain size in weathered and unweathered till. *Geol. Surv. Can. Pap. 85-1A* **1985**, 117–122. [CrossRef]
48. DiLabio, R.N.W. Residence sites of gold, PGE, and rare lithophile elements in till. In *Prospecting in Areas of Glaciated Terrain*; MacDonald, D.R., Mills, K.A., Eds.; Canadian Institute of Mining and Metallurgy: Montréal, QC, Canada, 1988; pp. 121–140.
49. Craw, D.P.; Upton, P.; Mackenzie, D.J. Hydrothermal alteration styles in ancient and modern orogenic gold deposits, New Zealand. *N. Z. J. Geol. Geophys.* **2009**, *52*, 11–26. [CrossRef]
50. Shelp, S.G.; Nichol, I. Distribution and dispersion of gold in glacial till associated with gold mineralization in the Canadian Shield. *J. Geochem. Explor.* **1987**, *27*, 315–336. [CrossRef]
51. Sopuck, V.J.; Schreiner, B.T.; Averill, S.A. Drift prospecting for gold in Saskatchewan-use of heavy mineral concentrates in tills. In *Gold in the Western Shield*; Clark, L.A., Ed.; Canadian Institute of Mining Metallurgy: Montréal, QC, Canada, 1986; Volume 38, pp. 435–469.
52. McClenaghan, M.B. Regional and local-scale gold grain and till geochemical signatures of lode Au deposits in the western Abitibi Greenstone Belt, central Canada. In *Drift Exploration in Glaciated Terrain*; McClenaghan, M.B., Bobrowsky, P.T., Hall, G.E.M., Cook, S.J., Eds.; Geological Society: London, UK, 2001; Volume 185, pp. 201–224. [CrossRef]
53. McClenaghan, M.B.; Plouffe, A.; McMartin, I.; Campbell, J.E.; Spirito, W.A.; Paulen, R.C.; Garrett, R.G.; Hall, G.E.M. Till sampling and geochemical analytical protocols used by the Geological Survey of Canada. *Geochem. Explor. Environ. Anal.* **2013**, *13*, 285–301. [CrossRef]
54. Néron, A.; Girard, R.; Bédard, L.P. *Automated Optical Gold Grain Counting: A Quantum Leap*; Annual Meeting, Abstract; Geological Association of Canada—Mineralogical Association of Canada: St-John's, NL, Canada, 2017.
55. Néron, A.; Girard, R.; Bédard, L.P. *ARTPhot: Automated Routine for Grain Counting Using a Digital Microscope and a Neural Network*; Annual Meeting, Abstract; Geological Association of Canada-Mineralogical Association of Canada: St-John's, NL, Canada, 2018.

56. Girard, R.; Tremblay, J.; Néron, A.; Longuépée, H. Automated gold grain counting: Part 3: The chemical footprint! *Minerals* **2021**. in preparation. [CrossRef]
57. Wang, W.; Poling, G.W. Methods for recovering fine placer gold. *Can. Inst. Min. Metall. Bull.* **1983**, *76*, 47–56.
58. Cabri, L.J.; Beattie, M.; Rudashevsky, N.S.; Rudashevsky, V.N. Process mineralogy of Au, Pd and Pt ores from the Skaergaard intrusion, Greenland, using new technology. *Miner. Eng.* **2005**, *18*, 887–897. [CrossRef]
59. Mitchell, C.J.; Evans, E.J.; Styles, M.T. *A Review of Gold Particle-Size and Recovery Methods*; British Geological Survey Technical Report WC/97/14; British Geological Survey: Nottingham, UK, 1997.
60. Clifton, H.E.; Hunter, R.E.; Swanson, F.J.; Philipps, R.L. *Sample Size and Meaningful Gold Analysis*; U.S. Geological Survey Professional Paper 625-C; S. Geological Survey: Washington, DC, USA, 1969; pp. C1–C17.
61. Grammatikopoulos, T.A.; Porritt, L.; Petersen, J.S.; Christensen, K. Mineralogical characterization and process mineralogy of gold bearing rocks from the Nalunaq gold deposit, Greenland. *Appl. Earth Sci.* **2004**, *113*, 197–203. [CrossRef]
62. Dominy, S.C.; Platten, I.M. Gold particle clustering: A new consideration in sampling applications. *Appl. Earth Sci.* **2007**, *116*, 130–142. [CrossRef]
63. Dominy, S.C.; O'Connor, L.; Glass, H.J.; Xie, Y. Geometallurgical study of a gravity recoverable gold orebody. *Minerals* **2018**, *8*, 186. [CrossRef]
64. Dominy, S.C.; Xie, Y.; Platten, I.M. Characterisation of in situ gold particle size and distribution for sampling protocol optimisation. In Proceedings of the Ninth International Congress for Applied Mineralogy, Brisbane, Australia, 8–10 September 2008; pp. 175–185.
65. Bergman, R.B.; Bill, A. On the origin of logarithmic-normal distributions: An analytical derivation and its application to nucleation and growth processes. *J. Cryst. Growth.* **2008**, *301*, 3135–3138. [CrossRef]
66. Healy, R.E.; Petruk, W. Petrology of Au-Ag-Hg alloy and "invisible" gold in the Trout Lake massive sulfide deposit, Flin Flon, Manitoba. *Can. Min.* **1990**, *28*, 189–206.
67. Sibbick, S.J.; Fletcher, W.K. Distribution and behavior of gold in soils and tills at the Nickel Plate Mine, southern British Columbia, Canada. *J. Geochem. Explor.* **1993**, *47*, 183–200. [CrossRef]
68. Brushett, D. Prospecting under cover: Using knowledge of glacial processes in mineral exploration. *Geol. Surv. Nfld. Labrador* **2014**, *5*, 2014.
69. Néron, A.; Madon, B.; Girard, R. *Volumetric Calculation of Minute Gold Grain: Insight from Machine Learning*; Annual Meeting Abstract; Geological Association of Canada-Mineralogical Association of Canada: St-John's, NL, Canada, 2019.
70. Néron, A.; Tremblay, J.; Girard, R. *Convolutional Neuron Network Image Classifier Optimized for Detection of Rare Geological Features: An Example on Gold Grains in Tills*; Annual Meeting, Abstract; Geological Association of Canada, Mineralogical Association of Canada: St-John's, NL, Canada, 2019.
71. Maitre, J.; Bouchard, K.; Bédard, L.P. Mineral grains recognition using computer vision and machine learning. *Comput. Geosci.* **2019**, *130*, 84–93. [CrossRef]
72. Youngson, J.H.; Craw, D. Variation in placer style, gold morphology, and gold particle behavior down gravel bed-load rivers: An example from the Shotover/Arrow-Kawarau-Clutha river system, Otago, New Zealand. *Econ. Geol.* **1999**, *94*, 615–634. [CrossRef]
73. Townley Brian, K.; Hérail, G.; Maksaev, V.; Palacios, C.; de Parseval, P.; Sepulveda, F.; Orellana, R.; Rivas, P.; Ulloa, C. Gold grain morphology and composition as an exploration tool: Application to gold exploration in covered areas. *Geochem. Explor. Environ. Anal.* **2003**, *3*, 29–38. [CrossRef]
74. Fominykh, P.A.; Nevolko, P.A.; Svetlitskaya, T.V.; Kolpakov, V.V. Native gold from the Kamenka-Barabanowsky and Kharuzovka alluvial placers (Northwest salair ridge, Western Siberia, Russia): Typomorphic features and possible bedrock sources. *Ore Geol. Rev.* **2020**, *126*, 103781. [CrossRef]
75. Liu, H.; Beaudoin, G.; Makvandi, S.; Jackson, S.E.; Huang, X. Multivariate statistical analysis of trace element compositions of native gold from orogenic gold deposits: Implication for mineral exploration. *Ore Geol. Rev.* **2021**, *131*, 104061. [CrossRef]
76. Dilabio, R.N.W.; Newsome, J.W.; McIvor, D.F.; Lowenstein, P.L. The spherical form of gold: Man-made or secondary? Geological Survey of Papua New Guinea, Volcanological Observatory, P.O Box 386, Rabaul, Papua New Guinea. *Econ. Geol.* **1988**, *83*, 153–168. [CrossRef]
77. Patel, H.; Jain, R.; Joshi, M.V. Automatic segmentation and yield measurement of fruit using shape analysis. *Int. J. Comput. Appl. Tech.* **2012**, *45*, 19–24.
78. Schneider, C.A.; Rasband, W.S.; Eliceiri, K.W. NIH Image to ImageJ: 25 years of image analysis. *Nat. Methods* **2012**, *9*, 671–675. [CrossRef]
79. Dürig, T.; Bowman, M.H.; White, J.D.L.; Murch, A.; Mele, D.; Verolino, A.; Dellino, P. Particle shape analyzer PARTISAN–An open-source tool for multi-standard two-dimensional particle morphometry analysis. *Ann. Geophys.* **2018**, *61*, 61–66. [CrossRef]
80. Paulen, R.C. Sampling techniques in the western Canada sedimentary basin and the Cordillera. In *Application of Till and Stream Sediment Heavy Mineral and Geochemical Methods to Mineral Exploration in Western and Northern Canada*; GAC Short Course Notes 18; Paulen, R.C., McMartin, I., Eds.; Geological Association of Canada: St-John's, NL, Canada, 2009; pp. 49–73.
81. Stea, R.; Johnson, M.; Hanchar, D. The geometry of kimberlitic indicator mineral dispersal fans in Nunavut, Canada. Référence sur les trainées palimpsestes, Parent. In *Application of Till and Stream Sediment Heavy Mineral and Geochemical Methods to Mineral Exploration in Western and Northern Canada*; GAC Short Course Notes 18; Paulen, R.C., McMartin, I., Eds.; Geological Association of Canada: St-John's, NL, Canada, 2009; pp. 1–13.

82. Hart, C.J.R. Reduced intrusion-related gold systems. In *Mineral Deposits of Canada: A Synthesis of Major Deposit Types, District Metallogeny, the Evolution of Geological Provinces, and Exploration Methods*; Goodfellow, W.D., Ed.; Mineral Deposits Division, Special Publication No. 5; Geological Association of Canada: St-John's, NL, Canada, 2007; pp. 95–112.
83. Hamilton, S.M. Electrochemical mass-transport in overburden: A new model to account for formation of selective leach geochemical anomalies in glaciated terrain. *J. Geochem. Explor.* **1998**, *63*, 155–172. [CrossRef]